

# **Development and Evaluation of Nanoscale Sorbents for Mercury Capture from Warm Fuel Gas**

## **Final Report**

September 27, 2004 – May 31, 2006

By

Raja A. Jadhav, Ph.D.  
Project Manager

August 25, 2006

## **Work Performed under Contract No. DE-FC26-04NT42312**

September 27, 2004 – May 31, 2006

For

U.S. Department of Energy, National Energy Technology Laboratory (NETL)  
Ronald Breault, Project Manager  
3610 Collins Ferry Road, P.O. Box 880  
Morgantown, WV 26507-0880

## **Submitted by**

Gas Technology Institute (GTI)  
1700 S. Mount Prospect Road  
Des Plaines, IL 60018

and

NanoScale Materials, Inc. (Subcontractor)  
1310 Research Park Dr.  
Manhattan, KS 66502

## **Technical Point of Contact**

Raja A. Jadhav, Ph.D.  
Engineer, GTI  
Phone: (847) 768-0807, Fax: (847) 768-0600  
E-mail: [raja.jadhav@gastechnology.org](mailto:raja.jadhav@gastechnology.org)

## **DISCLAIMER**

This report was prepared as an account of work sponsored by an agency of the United States Government. Neither the United States Government nor any agency thereof, nor any of their employees, makes any warranty, expressed or implied, or assumes any legal liability or responsibility for the accuracy, completeness, or usefulness of any information, apparatus, product, or process disclosed, or represents that its use would not infringe privately owned rights. Reference herein to any specific commercial product, process, or service by trade name, trademark, manufacturer, or otherwise does not necessarily constitute or imply its endorsement, recommendation, or favoring by the United States Government or any agency thereof. The views and opinions of authors expressed herein do not necessarily state or reflect those of the United States Government or any agency thereof.

## ABSTRACT

Several different types of nanocrystalline metal oxide sorbents were synthesized and evaluated for capture of mercury (Hg) from coal-gasifier warm fuel gas. Detailed experimental studies were carried out to understand the fundamental mechanism of interaction between mercury and nanocrystalline sorbents over a range of fuel gas conditions.

The metal oxide sorbents evaluated in this work included those prepared by GTI's subcontractor NanoScale Materials, Inc. (NanoScale) as well as those prepared in-house. These sorbents were evaluated for mercury capture in GTI's Mercury Sorbent Testing System. Initial experiments were focused on sorbent evaluation for mercury capture in N<sub>2</sub> stream over the temperature range 423–533 K. These exploratory studies demonstrated that NanoActive Cr<sub>2</sub>O<sub>3</sub> along with its supported form was the most active of the sorbent evaluated. The capture of Hg decreased with temperature, which suggested that physical adsorption was the dominant mechanism of Hg capture. Desorption studies on spent sorbents indicated that a major portion of Hg was attached to the sorbent by strong bonds, which suggested that Hg was oxidized by the O atoms of the metal oxides, thus forming a strong Hg—O bond with the oxide.

Initial screening studies also indicated that sulfided form of CuO/alumina was the most active for Hg capture, therefore was selected for detailed evaluation in simulated fuel gas (SFG). It was found that such supported CuO sorbents had high Hg-sorption capacity in the presence of H<sub>2</sub>, provided the gas also contained H<sub>2</sub>S. Exposure of supported CuO sorbent to H<sub>2</sub>S results in the formation of CuS, which is an active sorbent for Hg capture. Sulfur atom in CuS forms a bond with Hg that results into its capture. Although thermodynamically CuS is predicted to form unreactive Cu<sub>2</sub>S form when exposed to H<sub>2</sub>, it is hypothesized that Cu atoms in such supported sorbents are in “dispersed” form, with two Cu atoms separated by a distance longer than required to form a Cu<sub>2</sub>S molecule. Thus CuS remains in the stable reactive form as long as H<sub>2</sub>S is present in the gas phase. It was also found that the captured Hg on such supported sorbents could be easily released when the spent sorbent is exposed to a H<sub>2</sub>-containing stream that is free of Hg and H<sub>2</sub>S. Based on this mechanism, a novel regenerative process has been proposed to remove Hg from fuel gas at high temperature. Limited multicyclic studies carried out on the supported Cu sorbents showed their potential to capture Hg from SFG in a regenerative manner.

This study has demonstrated that supported nanocrystalline Cu-based sorbents have potential to capture mercury from coal syngas over multiple absorption/regeneration cycles. Further studies are recommended to evaluate their potential to remove arsenic and selenium from coal fuel gas.

## EXECUTIVE SUMMARY

Coal-fired utilities are the largest source of anthropogenic mercury emissions in the U.S. and are responsible for annual emission of nearly 43 tons of mercury. Because of the growing concern about the toxic effects of mercury on fish-eating population, on March 15, 2005, the U.S. EPA proposed Clean Air Mercury Rule for control of mercury emissions from coal-fired power plants. Gasification-based energy conversion systems, such as Integrated Gasification Combined Cycle (IGCC), are currently under development and have the potential to provide energy with higher efficiency and superior environmental performance. The mercury regulations proposed for coal-combustion systems will most likely be extended to these next-generation gasification-based systems. Therefore, the DOE has outlined goals of developing technologies that will reduce mercury emission 90% by 2010. To achieve that goal, the DOE has called for advanced research in the fundamental mechanisms affecting mercury control in fossil energy systems. One of its objectives is development of novel materials with potential to capture 100% mercury in post-gasification warm fuel gas.

With this objective in mind, Gas Technology Institute (GTI) proposed development of nanoscale materials with high surface area and higher reactivity, which would capture mercury from high-pressure (2–7 MPa) and high-temperature (420–640 K) fuel gas under reducing conditions and in the presence of other gases and particulate matter. GTI, in collaboration with Nanoscale Materials, Inc. (NanoScale), developed and evaluated several nanocrystalline sorbents for capture of mercury from coal-gasifier (such as IGCC) warm fuel gas. The focus of this study was on the understanding of fundamental mechanism of interaction between mercury and nanocrystalline sorbents over a range of fuel gas conditions. Detailed chemical and structural analysis of the sorbents were carried out using an array of experimental techniques to understand the mechanism of interaction between the sorbent and mercury.

Several different types of nanocrystalline metal oxides were synthesized by NanoScale. These included NanoActive® TiO<sub>2</sub>, CeO<sub>2</sub>, ZnO, CuO and NanoActive®-D MoO<sub>3</sub>, Cr<sub>2</sub>O<sub>3</sub>, and MnO<sub>2</sub>. Additionally, supported forms of selected metal oxides were synthesized by NanoScale. At GTI, supported CuO on alumina were synthesized by incipient wetness method, in addition to mixed metal oxides of the form Cu-Cr-O and Cu-Ce-O. These sorbents were evaluated for Hg capture in GTI's Mercury Sorbent Testing System. Detailed chemical and structural analysis of the sorbents were carried out using an array of techniques, such as thermal desorption, XRD, N<sub>2</sub>-adsorption, to understand the mechanism of interaction between the sorbent and mercury.

Initial experiments were focused on sorbent evaluation for mercury capture in N<sub>2</sub> stream over the temperature range 423–533 K. These exploratory studies demonstrated that NanoActive Cr<sub>2</sub>O<sub>3</sub> along with its supported form was the most active of the sorbent evaluated. The capture of Hg decreased with temperature, which suggested that physical adsorption was the dominant mechanism of Hg capture. Desorption studies on spent sorbents indicated that a major portion of Hg was attached to the sorbent by strong bonds, which suggested that Hg was oxidized by the O atoms of the metal oxides, thus forming a strong Hg—O bond with the oxide.

Based on the preliminary studies in N<sub>2</sub>, three metal oxides (NanoActive CuO, MnO<sub>2</sub>, and Cr<sub>2</sub>O<sub>3</sub>) were selected for detailed evaluation in simulated fuel gas (SFG). Initial studies focused on sorbent evaluation in H<sub>2</sub>/N<sub>2</sub> mixture. These studies indicated that H<sub>2</sub> had a negative effect on Hg-sorption capacities of the NanoActive sorbents. It is theorized that H<sub>2</sub> reacts with the metal oxides to form a reduced and unreactive form of the metal oxides. The active O atom in the

metal oxides is no longer available to interact with Hg when  $H_2$  is also present in the gas stream, resulting in drastically reduced sorbent capacities.

To explore the effect of  $H_2$  further, high surface area metal oxide sorbents were synthesized by depositing them on high surface area alumina supports. It was found that such supported CuO sorbents had high Hg-sorption capacity in the presence of  $H_2$ , provided the gas also contained  $H_2S$ . Exposure of supported CuO sorbent to  $H_2S$  results in the formation of CuS, which is an active sorbent for Hg capture. Sulfur atom in CuS forms a bond with Hg that results into its capture. Although thermodynamically CuS is predicted to form unreactive  $Cu_2S$  form when exposed to  $H_2$ , it is hypothesized that Cu atoms in such supported sorbents are in “dispersed” form, with two Cu atoms separated by a distance longer than required to form a  $Cu_2S$  molecule. Thus CuS remains in the stable reactive form as long as  $H_2S$  is present in the gas phase. It was also found that the captured Hg on such supported sorbents could be easily released when the spent sorbent is exposed to  $H_2$ -containing stream that is free (or lean) of Hg and  $H_2S$ . Limited multicyclic studies carried out on the supported Cu sorbents showed the potential of these sorbents to capture Hg from SFG in regenerative manner.

This experimental study has demonstrated that supported nanocrystalline Cu-based sorbents have a potential to capture mercury from coal fuel gas with high efficiency. Limited studies on supported forms of binary oxides of Cu and Cr have demonstrated their potential as effective Hg sorbents. Since CuS-based sorbents are known to capture arsenic as well, further studies are recommended to synthesize supported Cu-sorbents with higher Cu loadings and evaluate their potential to remove arsenic and selenium along with mercury from coal fuel gas in a regenerative manner.

## TABLE OF CONTENTS

ABSTRACT	ii
EXECUTIVE SUMMARY	iii
LIST OF TABLES	vi
LIST OF FIGURES	vii
1. Mercury Capture from Coal Fuel Gas at High Temperature	1
1.1 Introduction	1
1.2 Background Literature	1
1.3 Nanocrystalline Sorbents	2
Literature Cited	4
2. Shakedown Testing of the Experimental System	6
2.1 Introduction	6
2.2 Experimental Methods	6
2.3 Results and Discussion	6
2.4 Conclusions	8
3. Synthesis of Metal Oxide Sorbents	11
3.1 Introduction	11
3.2 Synthesis of Nanocrystalline Sorbents	11
3.2.1 Experimental Methods	11
3.2.2 Results and Discussion	12
3.3 Synthesis of Supported CuO Sorbents	16
3.3.1 Experimental Methods	16
3.3.2 Results and Discussion	16
3.4 Synthesis of Mixed Metal Oxide Sorbents	16
3.4.1 Experimental Methods	16
3.4.2 Results and Discussion	16
3.5 Conclusions	17
4. Preliminary Evaluation of Sorbents	20
4.1 Introduction	20
4.2 Experimental Methods	20
4.3 Results and Discussion	21
4.4 Conclusions	22
5. Sorbent Evaluation in Simulated Fuel Gas	27
5.1 Introduction	27
5.2 Experimental Methods	27
5.3 Results and Discussion	28
5.4 Conclusions	30
6. Overall Conclusions	36

## LIST OF TABLES

<u>Table</u>	<u>Page</u>
1.1 Sorbents proposed for this work and their rationale	4
3.1 Properties of pure NanoActive metal oxide sorbents	13
3.2 Properties of supported nanocrystalline MnO <sub>2</sub> sorbents	13
3.3 Properties of supported nanocrystalline Cr <sub>2</sub> O <sub>3</sub> sorbents	14
3.4 Properties of supported nanocrystalline CuO sorbents	14
4.1 Comparison of Hg-sorption capacities of NanoActive® sorbents	24

## LIST OF FIGURES

<u>Figure</u>	<u>Page</u>
2.1 Schematic of GTT's experimental setup for mercury sorbent testing	9
2.2 Mercury concentrations obtained from analyzer under different configurations	9
2.3 Mercury concentrations obtained from analyzer using two different sources of Hg	10
3.1 XRD spectra of NanoActive metal oxides	15
3.2 XRD spectra of developmental nanocrystalline metal oxides	15
3.3 XRD spectrum of 20 wt% Cu/alumina	18
3.4 XRD spectra of Cu-Cr-O (Top) and Cu-Ce-O (Bottom) binary oxides	19
4.1 Mercury breakthrough plot for NanoActive MnO <sub>2</sub> /alumina sorbent at 423 K	25
4.2 Adsorption/desorption studies on NanoActive MnO <sub>2</sub> sorbent	25
4.3 Adsorption/desorption studies on NanoActive Cr <sub>2</sub> O <sub>3</sub> sorbent	26
4.4 Mercury breakthrough plot for NanoActive CuO at 423 K	26
5.1 Mercury breakthrough plot for 20 wt% Cu/alumina sorbent at 473 K	31
5.2 Mercury breakthrough plot for NanoActive 5 wt% CuO/alumina sorbent at 473 K	31
5.3 Mercury breakthrough plot for NanoActive 5 wt% CuO/alumina sorbent at 533 K	32
5.4 Mercury breakthrough plot for NanoActive 5 wt% CuO/alumina sorbent at 423 K	32
5.5 Adsorption/desorption of Hg on 20 wt% Cu/alumina sorbent at 423 K	33
5.6 XRD spectrum of 20 wt% Cu/alumina after exposure to H <sub>2</sub> S/H <sub>2</sub> /N <sub>2</sub> stream at 473 K	33
5.7 Multicyclic Hg-sorption studies on NanoActive 5 wt% CuO/alumina	34
5.8 Mercury breakthrough plot for 5:5 wt% Cu:Cr/alumina sorbent at 473 K	34
5.9 Mercury breakthrough plot for 5:5 wt% Cu:Cr/alumina sorbent at 533 K	35



## Chapter 1

# Mercury Capture from Coal Fuel Gas at High Temperature

### 1.1 Introduction

Coal-fired utilities are the single largest source of anthropogenic mercury emissions in the U.S. Because of its high volatility, almost all the mercury present in coal is transformed into gas phase during combustion or gasification of coal. Control of mercury emissions from coal-fired power plants is a difficult task, in part due to its high volatility and its much lower concentration ( $5\text{--}20\ \mu\text{g}/\text{m}^3$ ) in a large volume of flue gas. In addition, depending on the type of coal and combustion conditions, a majority of mercury in the flue gas can exist in the elemental form ( $\text{Hg}^0$ ), which is more difficult to capture than its oxidized ( $\text{Hg}^{2+}$ ) or particulate ( $\text{Hg}^p$ ) forms. The oxidized form of mercury can interact with fly ash and can be captured in conventional flue gas desulfurization (FGD) systems (such as wet FGD systems), whereas, the particulate form can be captured in the particulate control devices (PCDs). However, the elemental form is insoluble in water and does not have much affinity for fly ash. Therefore, almost all of the elemental mercury in the flue gas escapes to the atmosphere.

### 1.2 Background Literature

Many technologies are currently under development for removal of mercury from post-combustion flue gases. These include, amongst others, injection of a sorbent (e.g., activated carbon) in the post-combustor duct region followed by its capture in a PCD, capture of oxidized mercury species in a FGD system, or oxidation across a SCR catalyst followed by its capture in a wet FGD system. These mercury control technologies are not directly applicable to coal gasifier systems because of the inherent differences in the plant layout, gaseous components, and other parameters. In addition, due to the reducing nature of gasifier fuel gas, mercury exists predominantly in the elemental form.<sup>1</sup> The lack of oxidized mercury in fuel gas is the result of higher concentrations of CO and  $\text{H}_2\text{S}$ , which inhibit mercury oxidation by scavenging the chlorine and other radicals necessary for mercury oxidation.<sup>2</sup> Activated carbon-based technology currently proposed for flue gas mercury control has limited application in fuel gas because of the lower sorption capacity of the activated carbon at elevated temperatures. The presence of reducing components in the fuel gas provides additional challenge for development of high capacity mercury sorbents for coal-gasifier applications.

High-pressure coal gasifiers, fortunately, present us with an opportunity to take advantage of the higher concentration of mercury in a much smaller fuel gas volume. Eastman Chemical Co.<sup>3</sup> has been practicing mercury removal from coal syngas using S-impregnated activated carbon (SIAC) beds at  $\sim 303\ \text{K}$  and  $7\ \text{MPa}$  with  $\sim 15\text{--}20\ \text{sec}$  of contact time. A detailed economic study carried out by Parsons indicates that mercury removal costs from such a process would be approx.  $\$3400/\text{lb}$  of Hg removed and would result in less than 1% rise in the cost of electricity (COE).<sup>4</sup> For similarly sized coal-combustion plant, the corresponding cost is estimated to be  $\$37,800/\text{lb}$  of Hg removed. The lower cost of Hg control for an IGCC plant is due to greatly reduced volumetric gas flow rate (by a factor of nearly 200), which also results in reduced size of the equipment, number of beds and other subsequent costs.<sup>4</sup>

Activated carbon-based processes are generally operated at lower temperatures to increase the sorbent capacity, as the capture is dependent on the physical interaction between carbon and mercury. Such low-temperature processes employing high surface area activated carbons (e.g.,

Eastman Chemical Co. process) or zeolites (e.g., UOP's HgSiv Process<sup>5</sup>) are ideally suited for coal gasifier systems where the syngas is used for chemicals production at lower temperatures. However, for IGCC systems, such processes result in severe energy penalty and reduced efficiency, as the pressurized fuel gas has to be reheated to the gas turbine temperature ( $> 573$  K) for electricity generation. Therefore, current focus is on developing sorbents for removal of mercury from warm fuel gas in the temperature range (420–650 K) and at high pressure (2–7 MPa).

Development of a sorbent-based process for IGCC systems is a major challenge and currently no proven technologies exist for the removal of trace levels of mercury from high-temperature fuel gas. Activated carbon-based sorbents remove mercury primarily by physisorption mechanism, and they are not effective at higher temperatures. In addition, exposure of impregnated sorbent to gas stream at high temperature has shown to release the active component (e.g. sulfur) in the gas stream, making the sorbent ineffective.<sup>6</sup> Another major issue is the presence of highly reactive hydrogen in the fuel gas, which can alter the chemical characteristics of an otherwise active sorbent, making it ineffective for mercury removal. In addition, the reaction or interaction of mercury with the active component in the sorbent may not be favorable in the presence of hydrogen. For example, the stability of HgS and HgSe mercury species in reducing gases has been shown to be very low at temperatures higher than 573 K.<sup>7</sup>

Many studies are underway that specifically target mercury removal at higher temperature from coal gasifier fuel gas. Recent work at TDA Research Inc. has identified a regenerable sorbent with 0.1 wt.% (approx.) mercury adsorption capacity at 533 K in simulated fuel gas (SFG).<sup>8</sup> Studies at DOE-NETL have focused on development of sorbents based on metals, their oxides, sulfides, and selenides.<sup>9, 10, 11</sup> Their mercury removal studies in the presence of nitrogen have identified few promising sorbents. The Amended Silicate™ sorbent developed by ADA Technologies, Inc. has shown mercury capacity in excess of 3 wt.% at a temperature of 680 K and 1.4 MPa pressure.<sup>12</sup> Togaki et al.<sup>13</sup> have studied mercury removal potential of activated carbon and iron oxide from fuel gas over the range of 353–450 K. Their studies indicated that mercury removal activity was accelerated by the presence of H<sub>2</sub>S. It was proposed that active sulfur-sites were generated on the sorbent surface in the presence of H<sub>2</sub>S, which in turn interacted with gas-phase mercury.

### 1.3 Nanocrystalline Sorbents

A review of the prior work indicates that there is still a need to develop highly reactive mercury sorbents that have a potential to remove other pollutants, such as H<sub>2</sub>S and As. A detailed understanding of sorbent-mercury interaction under realistic fuel gas conditions is also lacking in the literature. The prior work has focused on the development of “bulk” or “microcrystalline” sorbents described above. These “microscale” sorbents, however, have limited applicability in coal-gasifier fuel gas applications. As mentioned earlier, these sorbents become ineffective in highly reducing conditions. For example, H<sub>2</sub> reduces CuS to Cu<sub>2</sub>S, which has very limited reactivity towards mercury. To address this problem, two novel approaches were proposed in this work: (a) development of nanoscale sorbents and (b) development of binary metal oxide sorbents.

Nanocrystalline materials exhibit a wide array of remarkable chemical and physical properties, and they can be considered as new materials that bridge molecular and condensed matter. One of their remarkable properties is enhanced surface chemical reactivity (normalized for surface

area) toward incoming adsorbates, which is attributed to extremely large surface areas, small crystallite size, unique morphology and porous nature of the nanomaterials. Nanocrystalline materials often show reactivity that is not observed in bulk materials. Such unusual properties of these materials would make them effective sorbents for mercury removal from warm fuel gas. With the potential to capture  $\text{H}_2\text{S}$  (and possibly arsenic and selenium) along with mercury, these novel multifunctional sorbents are expected to reduce the overall costs of pollution control in gasification-based systems.

Based on the extensive literature review and prior experience, seven metal oxides (and their sulfides) were proposed for this work:  $\text{CuO}$ ,  $\text{ZnO}$ ,  $\text{TiO}_2$ ,  $\text{CeO}_2$ ,  $\text{MnO}_2$ ,  $\text{MoO}_3$ , and  $\text{Cr}_2\text{O}_3$ . In addition, two sorbents based on binary metal oxides ( $\text{Cu-Cr-O}$  and  $\text{Cu-Ce-O}$ ) were proposed. These nanoscale sorbents haven't been evaluated in the past for their potential to capture mercury. It was proposed that favorable structural characteristics of these nanoscale sorbents combined with their unusual chemical reactivities would make them much more effective mercury sorbents than the bulk sorbents. The rationale for sorbent selection is summarized in Table 1.1.

Of these sorbents, oxides of Mn, Mo, and Cr have demonstrated moderate-to-significant capacity for mercury capture from argon and air streams.<sup>9</sup> Sulfides of some of these oxides have substantial capacity towards gas phase mercury. For example,  $\text{CuS}$  has been used widely in removal of mercury from oil and natural gas.<sup>14, 15</sup>  $\text{CuS}$  reacts with mercury in the gas stream and forms stable  $\text{HgS}$  product.  $\text{CuS}$ -based sorbents have also been explored for their mercury-removal potential for coal-gasifier applications.<sup>11</sup>

Although the prior work has demonstrated the potential of metal oxides for Hg removal, as described above, many knowledge gaps still exist. This project was undertaken to fill the prior knowledge gaps by evaluating the potential of nanocrystalline metal oxide sorbents for mercury capture from warm fuel gas and understanding the fundamental capture mechanism.

**Table 1.1:** Sorbents proposed for this work and their rationale

Sorbent	Rationale for Selection
CuO	CuO was expected to react with H <sub>2</sub> S in the fuel gas and form CuS. Nanoscale CuS was expected to be an effective sorbent for mercury.
ZnO	ZnO was expected to react with H <sub>2</sub> S in the fuel gas and form ZnS. Nanoscale ZnS was expected to be effective sorbent for mercury.
TiO <sub>2</sub>	Nanoparticle form of this sorbent was expected to oxidize Hg and have activity for mercury.
CeO <sub>2</sub>	CeO <sub>2</sub> was expected to oxidize Hg. In addition, when combined with CuO, it was expected to form Ce <sub>2</sub> S <sub>3</sub> in H <sub>2</sub> S, a possible Hg sorbent. <sup>16</sup>
MnO <sub>2</sub>	MnO <sub>2</sub> showed significant affinity towards mercury. <sup>9, 10, 11</sup> Nanoscale MnO <sub>2</sub> and its sulfided form was expected to have higher capacity and faster kinetics towards Hg.
MoO <sub>3</sub>	MoO <sub>3</sub> and MoS <sub>2</sub> showed significant affinity towards mercury. <sup>11</sup> Nanoparticle form of this sorbent was expected to have higher capacity and faster kinetics towards Hg.
Cr <sub>2</sub> O <sub>3</sub>	Cr <sub>2</sub> O <sub>3</sub> showed significant oxidation activity for mercury. <sup>9, 11</sup> Nanoparticle form of this sorbent was expected to have higher capacity and faster kinetics towards Hg.
CuO-Cr <sub>2</sub> O <sub>3</sub>	It was expected that Cr would suppress the reduction of Cu in the presence of H <sub>2</sub> and would maintain Cu in Cu <sup>2+</sup> state, <sup>16</sup> which would have enhanced reactivity towards Hg.
CuO-CeO <sub>2</sub>	It was expected that Ce would form Ce <sub>2</sub> S <sub>3</sub> in the presence of H <sub>2</sub> S and H <sub>2</sub> , <sup>16</sup> which in turn would react with Hg.

## Literature Cited

---

1. Reed, G.P., A. Ergudenler, J.R. Grace, A.P. Watkinson, A.A. Herod, D. Dugwell, and R. Kandiyoti, Control of gasifier mercury emissions in a hot gas filter: the effect of temperature, *Fuel*, **80**, 623-634, 2001.
2. Lu, D.Y., D.L. Granatstein, and D.J. Rose, A study of mercury speciation from simulated coal gasification, in Proc. of Combustion Canada '03 Conference, Vancouver, BC, 2003.
3. Denton, D.L., Eastman coal gasification: industry-leading performance and a demonstrated syngas mercury removal process, in Proceedings of Air Quality-III Conference: Mercury, Trace Elements and Particulate Matter, Arlington, VA, September 9-12, 2002.
4. Parsons Infrastructure and Technology Group Inc., The Cost of Mercury Removal in an IGCC Plant, Final Report to DOE/NETL, September 2002.
5. UOP, Presented at SAIC meeting: Environmental Performance/Issues of Gasification-based Power Systems, McLean, VA, July 12, 2001.

- 
6. Lopez-Anton, M.A., J.M.D. Tascon, and M.R. Martinez-Tarazona, Retention of mercury in activated carbons in coal combustion and gasification flue gases, *Fuel Process. Technol.*, **77-78**, 353-358, 2002.
  7. Benson, S.A., M.L. Swanson, and E.S. Olson, Trace element transformations and options for control in gasification systems, in Proceedings of Air Quality-III Conference: Mercury, Trace Elements and Particulate Matter, Arlington, VA, September 9-12, 2002.
  8. Alptekin, G., J. Monroe, R. Amalfitano, and R. Copeland, Sorbents for mercury removal from coal-derived synthesis gas, in Proceedings of Twentieth Annual International Pittsburgh Coal Conference, Pittsburgh, PA, September 15-19, 2003.
  9. Granite, E.J., H.W. Pennline, and R.C. Hargis, Novel sorbents for mercury removal from flue gas, *Ind. Eng. Chem. Res.*, **39**(4), 1020–1029, 2000.
  10. Granite, E.J., W.P. King, and H.W. Pennline, Techniques for mercury control and measurement in gasification systems, Presented at the 5th International Symposium on Gas Cleaning and High Temperature, Morgantown, WV, September 2002.
  11. Granite, E.J., W.P. King, and H.W. Pennline, Novel sorbents for mercury capture from fuel gas, Presented at the 20th Annual International Pittsburgh Coal Conference, Pittsburgh, PA, September 18, 2003.
  12. Butz, J.R., J.S. Lovell, T.E. Broderick, R.W. Sidwell, and C.S. Turchi, Evaluation of Amended Silicate™ sorbents for mercury control, in Proceedings of AWMA's Combined Power Plant Air Pollutant Control Mega Symposium, Washington, DC, May 19-22, 2003.
  13. Togaki, N., M.A. Uddin, W. Nakasima, S. Wu, S. Nagamine, and E. Sasaoka, Activity of adsorbents for removal of mercury vapor with H<sub>2</sub>S, in Proceedings of Twentieth Annual International Pittsburgh Coal Conference, Pittsburgh, PA, September 15-19, 2003.
  14. Yan, T.Y., Mercury removal from oil by reactive adsorption, *Ind. Eng. Chem. Res.*, **35**(10), 3697-3701, 1996.
  15. Sugier et al., Process for removing mercury from a gas or a liquid by absorption on a copper sulfide containing solid mass, US Patent # 4,094,777, June 1978.
  16. Li, Z, and M. Flytzani-Stephanopoulos, Cu-Cr-O and Cu-Ce-O regenerable oxide sorbents for hot gas desulfurization, *Ind. Eng. Chem. Res.*, **36**(1), 187-196, 1997.

## Chapter 2

### Shakedown Testing of the Experimental System

#### 2.1 Introduction

The Mercury Testing Experimental System available in GTI's Hot Gas Cleanup laboratory was prepared for the project. As part of the shakedown testing, the system was checked for possible gas leaks and fixed. In addition, the mass flow controllers were calibrated for diluent N<sub>2</sub> stream. A major part of the shakedown testing was the calibration of the semi-continuous mercury analyzer and the verification of the permeation rate of the mercury permeation tube.

#### 2.2 Experimental Methods

As part of this task, the mercury sorbent testing system shown in Figure 2.1 was checked for leaks and the mass flow controllers (MFC) were calibrated. In addition, the mercury permeation tube was calibrated using the P S Analytical (PSA) Sir Galahad-II Mercury Analyzer.

The leak check was performed by verifying the flow rate of N<sub>2</sub> at different locations in the experimental system. A flow rate of 3 lpm N<sub>2</sub> was used for the leak checks and the flow rate was measured using a digital flow meter. Any drop in the flow rate would indicate a possible leak in the system. Calibration of the MFCs were performed using a soap film meter and a stopwatch.

A major effort was focused on calibrating and checking the performance of the mercury analyzer. A mercury permeation tube obtained from VICI Metronics as part of an earlier program was used for these tests. The permeation tube was maintained at a constant temperature of 343 K in a water bath with 0.4 lpm of N<sub>2</sub> stream flowing over the tube. The tube was calibrated to deliver 522 ng/min of elemental Hg at 343 K. Therefore, about 174  $\mu\text{g}/\text{m}^3$  of Hg was expected when diluted in 3 lpm of total N<sub>2</sub> stream. As part of the testing, the mercury stream (0.4 lpm) was either bypassed or sent through the reactor. A diluent stream of 2.6 lpm of N<sub>2</sub> was always sent through the reactor.

#### 2.3 Results and Discussion

*Leak Checks:* A minor leak was found in the bottom section of the quartz reactor shell. The leak was fixed by applying a lubricant and tightening the reactor cap. No other leaks were found.

*MFC Calibration:* The MFC used for sending diluent N<sub>2</sub> stream to the reactor was calibrated using a soap-film meter. For the mercury sorption experiments, 0.4 lpm of Hg is mixed with 2.6 lpm of the diluent N<sub>2</sub> stream. As part of the calibration, it was found that 25% setting on the MFC delivered 2.6 lpm of N<sub>2</sub>. This setting of the MFC will be used for all the experiments to be carried out in Hg/N<sub>2</sub> stream.

*Mercury Analyzer Calibration:* The mercury testing system consists of Teflon® tubing and quartz reactor tube, both of which do not have any affinity for elemental mercury, even at room temperature. Therefore, the loss of mercury in the reactor system can be assumed negligible. The mercury analyzer has two separate channels to analyze both elemental and oxidized mercury. Since only elemental mercury was sent to the analyzer in this case, both the channels are expected to show similar mercury readings.

Figure 2.2 shows a plot of mercury concentration obtained in various configurations. Initially, 0.4 lpm of Hg-laden N<sub>2</sub> stream bypassed the reactor, and was mixed and diluted with 2.6 lpm of N<sub>2</sub> at the reactor exit and sent to the analyzer. Bypassing the reactor eliminated any possibility

of mercury loss in the reactor system. The analyzer showed nearly  $130 \mu\text{g}/\text{m}^3$  of Hg when the Hg/N<sub>2</sub> stream bypassed the reactor. This reading appeared to decrease slowly with time. When the Hg was sent through the reactor, nearly the same reading for Hg concentration was observed. After one and half hours, the mercury concentration appeared to be stable around  $125 \mu\text{g}/\text{m}^3$ . The difference between the two Hg channels was also negligible.

Next, the reactor was heated to 423 K to determine any effect of temperature on the Hg concentration. As shown in the figure, the Hg concentration of  $120 \mu\text{g}/\text{m}^3$  was obtained. After this, the Hg stream was sent to the vent to obtain a blank reading. Next, the above procedure was repeated to obtain Hg concentration for both the bypass and through-reactor configurations. The figure shows that for both these configurations, about  $120 \mu\text{g}/\text{m}^3$  of Hg concentration was obtained.

Based on these studies, it can be concluded that there is no noticeable effect of the quartz reactor (as well as its temperature) on the mercury concentration in the gas stream. It also appears that some time should be allowed to get a stable Hg reading.

The PSA analyzer showed a lower value of  $120 \mu\text{g}/\text{m}^3$  for the permeation tube that was calibrated for  $174 \mu\text{g}/\text{m}^3$ . Loss of elemental mercury in the transport tubing and reactor was not possible as the entire contact surface was either Teflon® or quartz, both of which are inert towards elemental mercury.

It was thought that the calibration of the permeation tube was no longer valid, being in use for more than 2 years. The manufacturer of the permeation tube was contacted to perform a recalibration. The vendor re-certified that the permeation rate of the tube decreased from the original certified value of 522 ng/min (+/- 2%) to 431 ng/min (+/- 2%) at 343 K. The re-certified permeation rate in 3 lpm N<sub>2</sub> stream corresponds to Hg concentration of approx.  $144 \mu\text{g}/\text{m}^3$ .

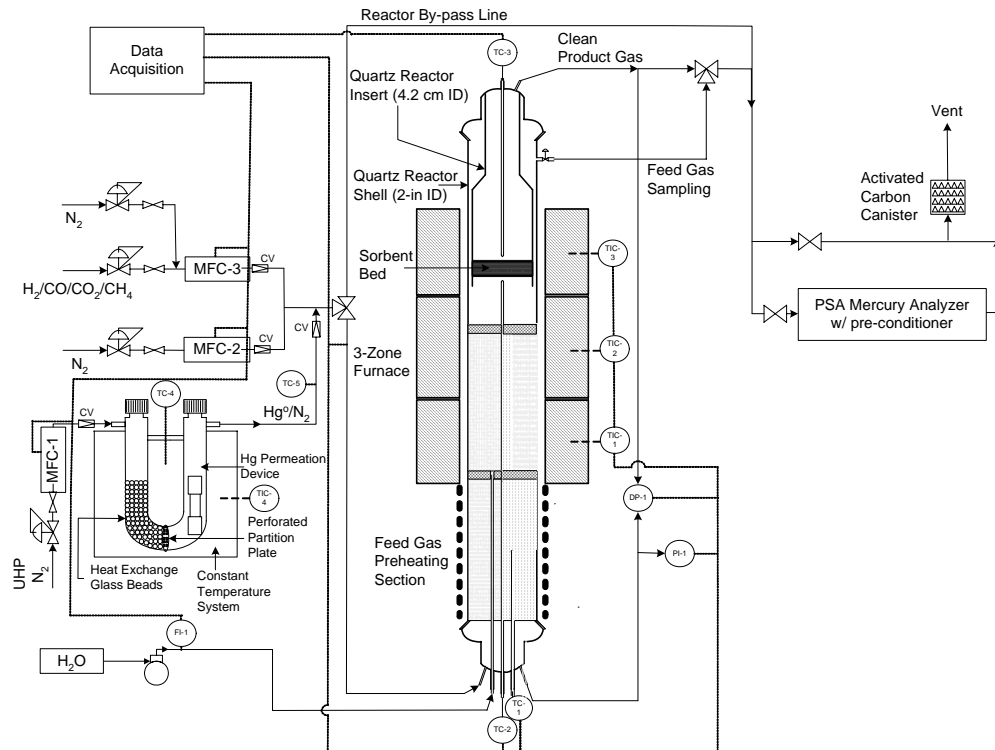
To confirm the reliability and performance of the mercury analyzer and the permeation tube, a Mercury Vapor Generator (MVG), designed to generate an accurate concentration of mercury, was obtained from PSA. The settings on the MVG were adjusted to deliver a stream containing  $62 \mu\text{g}/\text{m}^3$  of Hg in nitrogen. Figure 2.3 shows the performance of the analyzer when this Hg stream was sent to the analyzer. The figure also shows the mercury concentration when the permeation tube was used as a mercury source.

Figure 2.3 shows that when the MVG was used as the source of mercury, the analyzer showed  $66 \mu\text{g}/\text{m}^3$  as the concentration of mercury, close to the certified value of the MVG. When the permeation tube was used as the mercury source,  $140 \mu\text{g}/\text{m}^3$  was obtained as the concentration of mercury. As indicated above, the certified value of the permeation tube was  $174 \mu\text{g}/\text{m}^3$ . Earlier, as shown in Figure 2.2, a lower value of  $120 \mu\text{g}/\text{m}^3$  was obtained for the same permeation tube. For the experiment in Figure 2.3, the analyzer was recalibrated and the Hg stream was sent directly to the inlet of the analyzer, bypassing the impingers. Sending the Hg stream through the impingers possibly caused small pressure drop that resulted in lower flows on the mercury collection tube of the analyzer. These data indicate that the analyzer should be calibrated more frequently and the effect of impingers should be taken into consideration.

## **2.4 Conclusions**

The Mercury Sorbent Testing system available in GTI's Hot Gas Cleanup laboratory was found suitable for evaluating nanoscale mercury sorbents. As part of the initial shakedown testing, minor leaks observed in the system were fixed. The MFCs were also calibrated and found to perform well. A detailed testing of the mercury analyzer and the permeation tube was carried out. It was found that the re-certified permeation rate of the mercury tube was in close agreement with the value given by the mercury analyzer.





**Figure 2.1:** Schematic of GTI's experimental setup for mercury sorbent testing

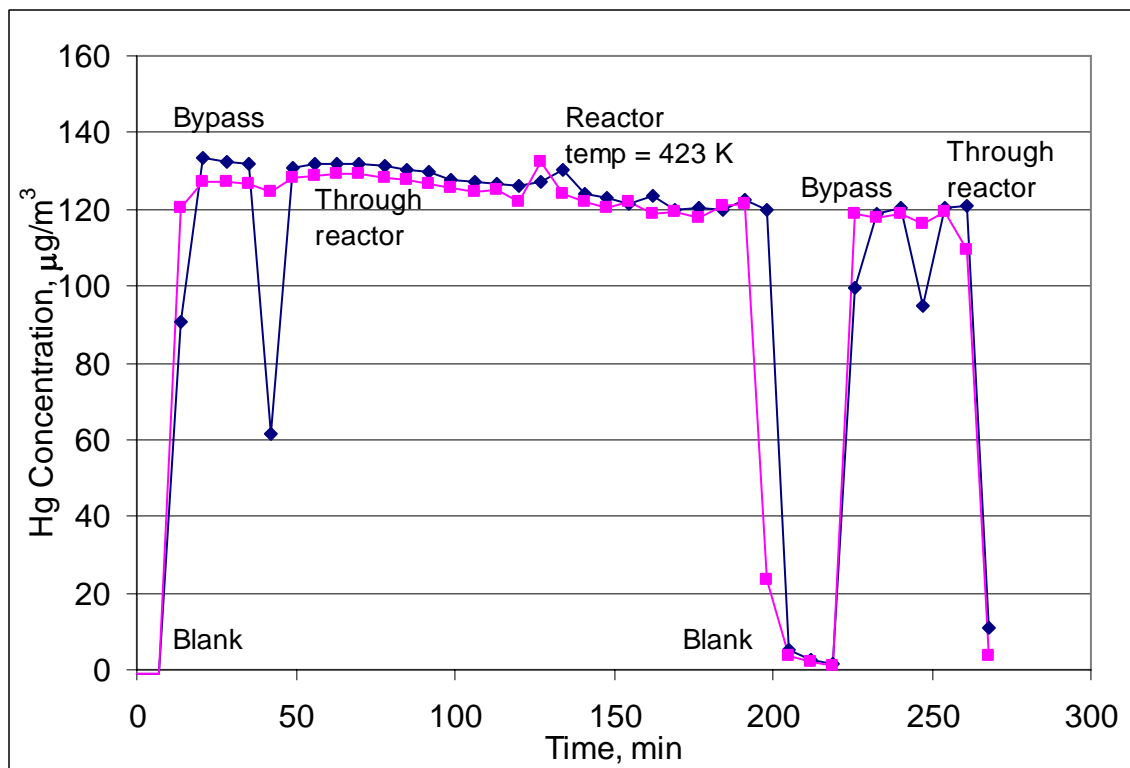


**Figure 2.2:** Mercury concentrations obtained from analyzer under different configurations

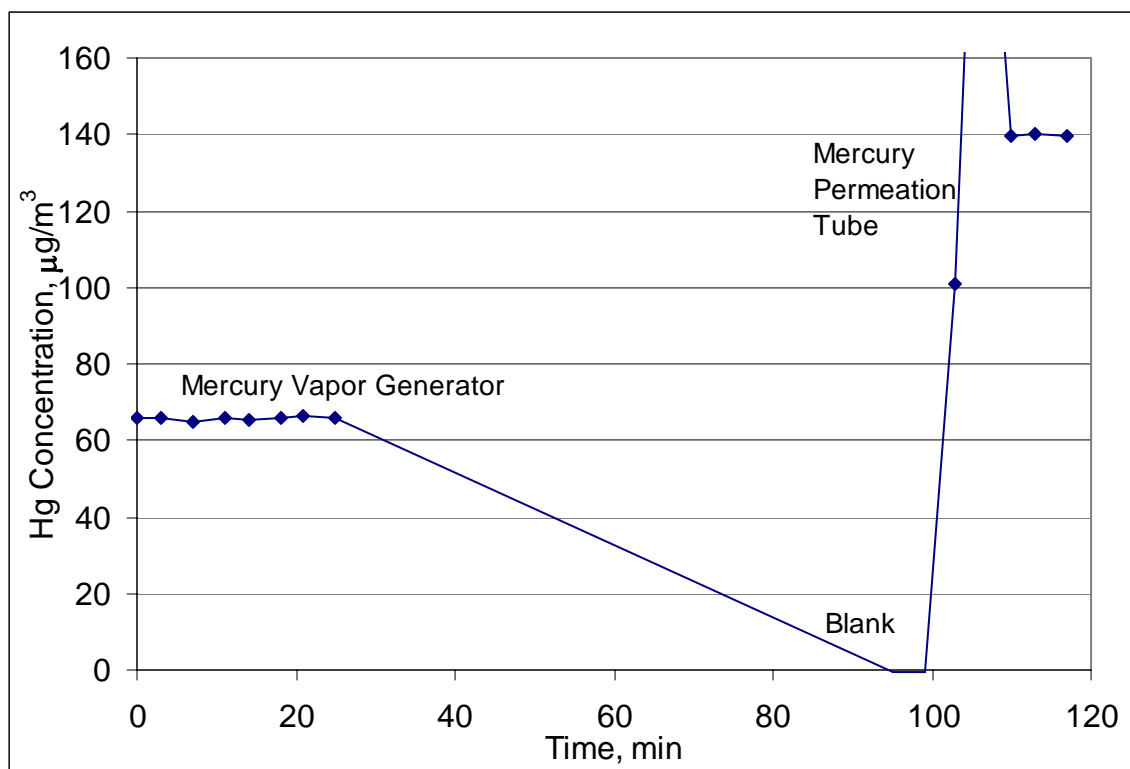


**Figure 2.3:** Mercury concentrations obtained from analyzer using two different sources of Hg

## Chapter 3

### Synthesis of Metal Oxide Sorbents

#### 3.1 Introduction

Several different types of nanocrystalline metal oxides were synthesized by subcontractor NanoScale Materials, Inc. (NanoScale). Additionally, supported forms of selected metal oxides were synthesized by NanoScale. At GTI, supported CuO on alumina were synthesized by incipient wetness method, in addition to mixed metal oxides of the form Cu-Cr-O and Cu-Ce-O. Detailed chemical and structural analysis of the fresh sorbents were carried out using an array of techniques, such as X-ray diffraction (XRD) and N<sub>2</sub>-adsorption.

#### 3.2 Synthesis of Nanocrystalline Sorbents

##### 3.2.1 Experimental Methods

###### *Synthesis of Sorbents*

NanoScale synthesized a total of seventeen sorbent formulations, including four existing sorbent formulations (NanoActive™ TiO<sub>2</sub>, NanoActive CeO<sub>2</sub>, NanoActive ZnO, and NanoActive CuO), three developmental nanocrystalline metal oxides (MnO<sub>2</sub>, MoO<sub>3</sub>, and Cr<sub>2</sub>O<sub>3</sub>), and ten supported forms of metal oxides. All formulations were synthesized by NanoScale using proprietary methods. The nanomaterials were pelletized by pressure-compaction method and ground to the desired size range (180–250 μm).

###### *Characterization of Sorbents*

Specific surface areas, total pore volumes and average pore diameters were determined using a *Quantachrome* Nova 2200 BET instrument. During the measurement nitrogen gas is applied to the sample, which is immersed in a liquid nitrogen bath. The amount of nitrogen adsorbed is measured as a function of nitrogen pressure. The resulting adsorption isotherm is analyzed according to the Brunauer, Emmett, and Teller (BET) method.

Chemical composition and crystallite size of metal oxide samples were determined using powder X-ray diffraction (XRD, *Kratos XDS-6000*). Using this technique, it is possible to determine if a powder is a pure metal oxide, or a mixture of different forms. In addition, the crystallinity of the sample can be determined as well as the lattice strain. To determine the crystallite size, the Scherrer equation is used:

$$\beta = K \lambda / L \cos \theta$$

where:  $\beta$  is the “physical half-value width” (in degrees  $2\theta$ ),  $L$  is the crystallite size (dimension of the crystallite perpendicular to the diffracting net planes),  $K$  is a constant (often taken as 0.9) and  $\lambda$  is the wavelength of the radiation employed. Materials prepared by NanoScale Materials have crystallite sizes in the range 2-25 nm.

Mechanical strength and resistance to vibration of granulated sorbents were evaluated using the ball pan hardness method, as defined in the ASTM D3802 standard. In this test, granulated material is placed on vibrating metal sieves for a fixed amount of time (30 minutes). The fraction of granules that remains on a metal sieve and does not break into smaller particles or powder, defines the ball pan hardness. The ball pan hardness test was performed only for three NanoActive metal oxides that were available in quantities required for this testing.

### 3.2.2 Results and Discussion

#### *Characterization of Nanocrystalline Sorbents*

Table 3.1 provides selected properties of pure metal oxide formulations prepared by NanoScale. Figures 3.1 and 3.2 present the XRD spectra of these materials. Tables 3.2, 3.3 and 3.4 display selected properties of supported forms of  $\text{MnO}_2$ ,  $\text{Cr}_2\text{O}_3$ , and  $\text{CuO}$ , respectively.

These structural and chemical properties indicate that the sorbents synthesized by NanoScale are nanocrystalline in nature and have high surface area.

**Table 3.1:** Properties of pure NanoActive metal oxide sorbents

Sorbent, lot #, appearance	Specific surface area, (m <sup>2</sup> /g)	Total pore volume (cc/g)	Average pore diameter (nm)	XRD crystallite, size (nm)	Ball-pan hardness, (%)
NanoActive TiO <sub>2</sub> , 312-0001, white granules	470	0.4	3.2	amorphous material	81
NanoActive CeO <sub>2</sub> , 306-0001, yellow granules	125	0.1	7	7	31
NanoActive ZnO, 305-0001, off-white granules	85	0.2	17	10	38
NanoActive CuO, 00-0104, black granules	45	0.1	8.5	8.1	N/A
Nanocrystalline MnO <sub>2</sub> , 0151-007 black granules	38	N/A	N/A	8.6	N/A
Nanocrystalline MoO <sub>3</sub> , 500-3-041305 Grey-blue granules	65	N/A	N/A	16	N/A
Nanocrystalline Cr <sub>2</sub> O <sub>3</sub> , D105-621 green granules	103	N/A	N/A	21	N/A

N/A – data not available

**Table 3.2:** Properties of supported nanocrystalline MnO<sub>2</sub> sorbents

Sorbent, lot #, appearance	Specific surface area, (m <sup>2</sup> /g)	XRD crystallite size, (nm)
Nanocrystalline MnO <sub>2</sub> supported on Al <sub>2</sub> O <sub>3</sub> (5 wt% loading), D110-625 brown granules	290	Amorphous material
Nanocrystalline MnO <sub>2</sub> supported on SiO <sub>2</sub> (5 wt% loading), D110-624 brown granules	154	Amorphous material
Nanocrystalline MnO <sub>2</sub> supported on SiO <sub>2</sub> (30 wt% loading), D110-623 brown granules	133	Amorphous material

**Table 3.3:** Properties of supported nanocrystalline Cr<sub>2</sub>O<sub>3</sub> sorbents

Sorbent, lot #, appearance	Specific surface area, (m <sup>2</sup> /g)	XRD crystallite size, (nm)
Nanocrystalline Cr <sub>2</sub> O <sub>3</sub> supported on Al <sub>2</sub> O <sub>3</sub> (30 wt% loading), D105-091205 light green granules	230	~18 (Cr <sub>2</sub> O <sub>3</sub> component)
Nanocrystalline Cr <sub>2</sub> O <sub>3</sub> supported on Al <sub>2</sub> O <sub>3</sub> (30 wt% loading), D105-092205 light green granules	230	Amorphous material
Nanocrystalline Cr <sub>2</sub> O <sub>3</sub> supported on Al <sub>2</sub> O <sub>3</sub> (30 wt% loading), D105-092305 light green granules	220	Amorphous material

**Table 3.4:** Properties of supported nanocrystalline CuO sorbents

Sorbent, lot #, appearance	Specific surface area, (m <sup>2</sup> /g)	XRD crystallite size, (nm)
Nanocrystalline CuO supported on Al <sub>2</sub> O <sub>3</sub> (5 wt% loading), D122-110105 brown granules	370	20 (CuO component)
Nanocrystalline CuO supported on Al <sub>2</sub> O <sub>3</sub> (5 wt% loading), D122-110205 brown granules	302	~20 (CuO component)
Nanocrystalline CuO supported on SiO <sub>2</sub> (6.5 wt% loading), D122-122905 blue-gray granules	290	~18 (CuO component)
Nanocrystalline CuO supported on ZnO (3 wt% loading), D122-010306 gray granules	24	~25 (CuO component)

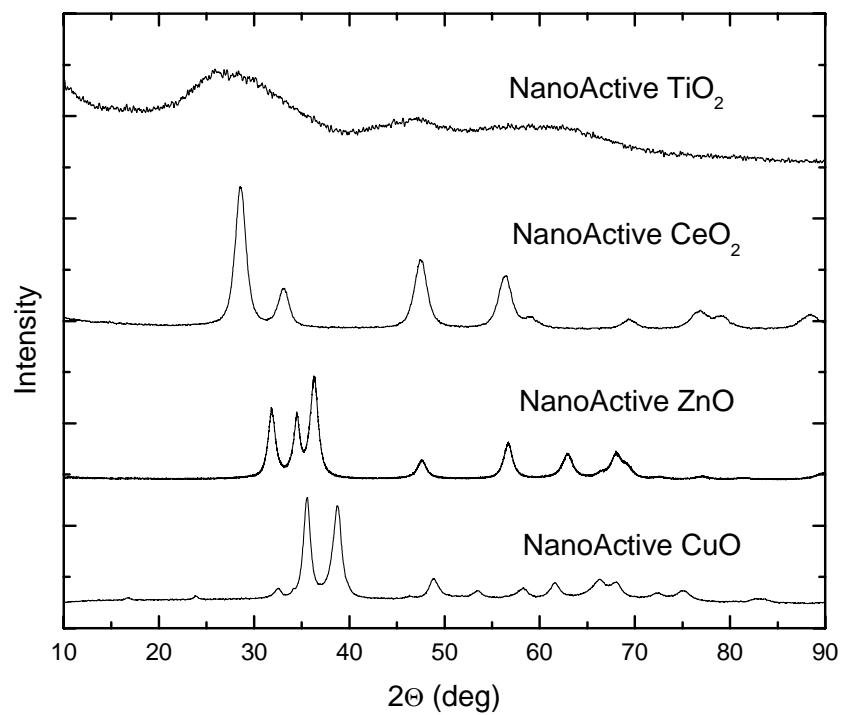


**Figure 3.1:** XRD spectra of NanoActive metal oxides

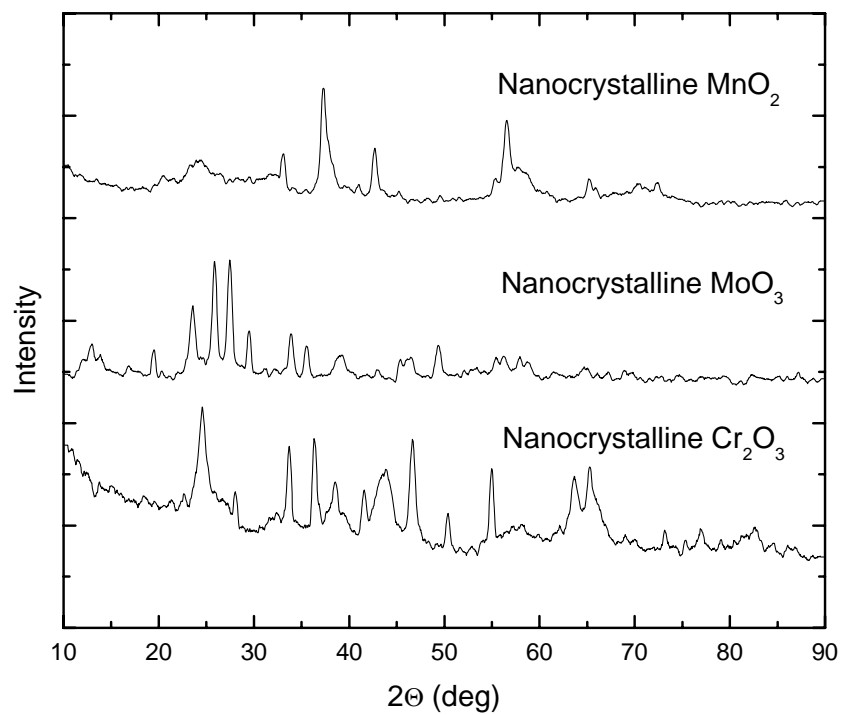


**Figure 3.2:** XRD spectra of developmental nanocrystalline metal oxides

### 3.3 Synthesis of Supported CuO Sorbents

#### 3.3.1 Experimental Methods

Several supported CuO sorbents were prepared at GTI. Alumina support pellets (1/8" size) with a surface area of 255 m<sup>2</sup>/g and pore volume of 1.14 cm<sup>3</sup>/g were obtained from Alfa-Aesar. The  $\gamma$ -alumina support had a bimodal pore size distribution with median pore sizes of 70  $\mu$ m and 500 nm. The support was chosen because of its high surface area and pore volume.

Incipient wetness method was used to prepare CuO sorbents with Cu loadings in the range 5–30 wt% on alumina. Copper nitrate was used as the source of copper. The prepared sorbents were dried at 384 K for 6 h and calcined in air at 673 K for 6 h to obtain CuO/alumina sorbents. The pellets were next crushed and sieved to obtain particles in the range 250–425  $\mu$ m. Although these Cu-sorbents were prepared in the oxide form, they are denoted here based on the loading of Cu metal on the support. For example, a 20 wt% Cu/alumina sorbent means a CuO sorbent with Cu loading of 20 wt% on alumina.

#### 3.3.2 Results and Discussion

XRD spectrum of 20 wt% Cu/alumina is shown in Figure 3.3. For such a supported sorbent, Cu was expected to be in the “dispersed” or “monolayer” form and the crystalline form of CuO was not expected. The presence of crystalline CuO in the figure suggests that some amount of Cu was loaded onto the support in multiple layers that gave rise to the crystalline structure of CuO during the calcination stage.

### 3.4 Synthesis of Mixed Metal Oxide Sorbents

#### 3.4.1 Experimental Methods

##### *Synthesis of Unsupported Binary Oxides*

Binary metal oxides Cu-Cr-O and Cu-Ce-O were prepared from amorphous citrate precursors according to a procedure given by Li et al.<sup>1</sup> To synthesize the oxides, an aqueous solution of cerium or chromium nitrate was mixed with a copper nitrate solution in 1:1 molar ratio. The mixed solution was then added dropwise into an aqueous solution of citric acid under continuous stirring at room temperature. The final solution was dehydrated rapidly in a rotary evaporator at 343 K under vacuum, and the resulting viscous solution was slowly dehydrated in a vacuum oven at 343 K. The resulting porous solid foam was calcined in a furnace at 1273 K for 1 h to obtain the binary mixed metal oxide sorbent. The synthesized binary metal oxides were analyzed for crystal structure using X-ray diffraction (XRD) and for surface area using the BET or N<sub>2</sub> adsorption method.

##### *Synthesis of Supported Binary Oxides*

Binary metal oxides of Cu and Cr were also prepared in the supported form using the incipient wetness method. A high surface area alumina support was used, as in the case of CuO sorbents. Nitrates of copper and chromium were used as the sources of the metals and their amounts in the solution were adjusted to give 5:5 wt% Cu:Cr on alumina.

#### 3.4.2 Results and Discussion

Synthesized Cu-Cr-O and Cu-Ce-O binary metal oxides were analyzed using XRD to determine the crystal structure of the sorbents. The spectra of these two sorbents are shown in Figure 3.4.



The XRD plots in Figure 3.4 indicate that for the equimolar CuO-Cr<sub>2</sub>O<sub>3</sub> material, copper chromite (CuCr<sub>2</sub>O<sub>4</sub>) was the only crystallite phase formed. Separate CuO and Cr<sub>2</sub>O<sub>3</sub> phases were not identified in the XRD plot. However, for the CuO-CeO<sub>2</sub> material, the XRD plot shows that separate CuO and CeO<sub>2</sub> phases were formed and no compound was formed during the synthesis.

The crystallite size of the synthesized particles was calculated using the Scherrer formula based on the line broadening in the XRD plot. Using this formula, crystallite size of CuCr<sub>2</sub>O<sub>4</sub> particles was ~ 34 nm. Crystallite sizes of the CuO and CeO<sub>2</sub> phases in the CuO-CeO<sub>2</sub> material were 45 and 47 nm, respectively.

The surface areas of the binary oxides were determined using the BET method, which gave surface areas of 2.2 m<sup>2</sup>/g for CuO-Cr<sub>2</sub>O<sub>3</sub> and 1.2 m<sup>2</sup>/g for CuO-CeO<sub>2</sub> material.

### 3.5 Conclusions

Several nanocrystalline sorbents were synthesized by GTI's subcontractor NanoScale Materials, Inc. (NanoScale). Additionally supported forms of selected metal oxides and mixed metal oxides were prepared at GTI. These sorbents were characterized for physical and chemical properties using a variety of analytical equipments, which confirmed their chemical form and nanocrystalline structure.

Nanocrystalline binary metal oxides with composition of Cu-Cr-O and Cu-Ce-O were synthesized using literature methods. XRD analysis of these materials indicated that CuCr<sub>2</sub>O<sub>4</sub> compound was formed from equimolar CuO and Cr<sub>2</sub>O<sub>3</sub>. For the equimolar CuO and CeO<sub>2</sub> material, however, separate CuO and CeO<sub>2</sub> phases were formed. The BET surface areas of these two sorbents were found to be low compared to the single-component nanomaterials.

### Literature Cited

---

1. Li, Z. and M. Flytzani-Stephanopoulos, Cu-Cr-O and Cu-Ce-O regenerable oxide sorbents for hot gas desulfurization, *Ind. & Eng. Chem. Res.*, **36**, 187-196, 1997.

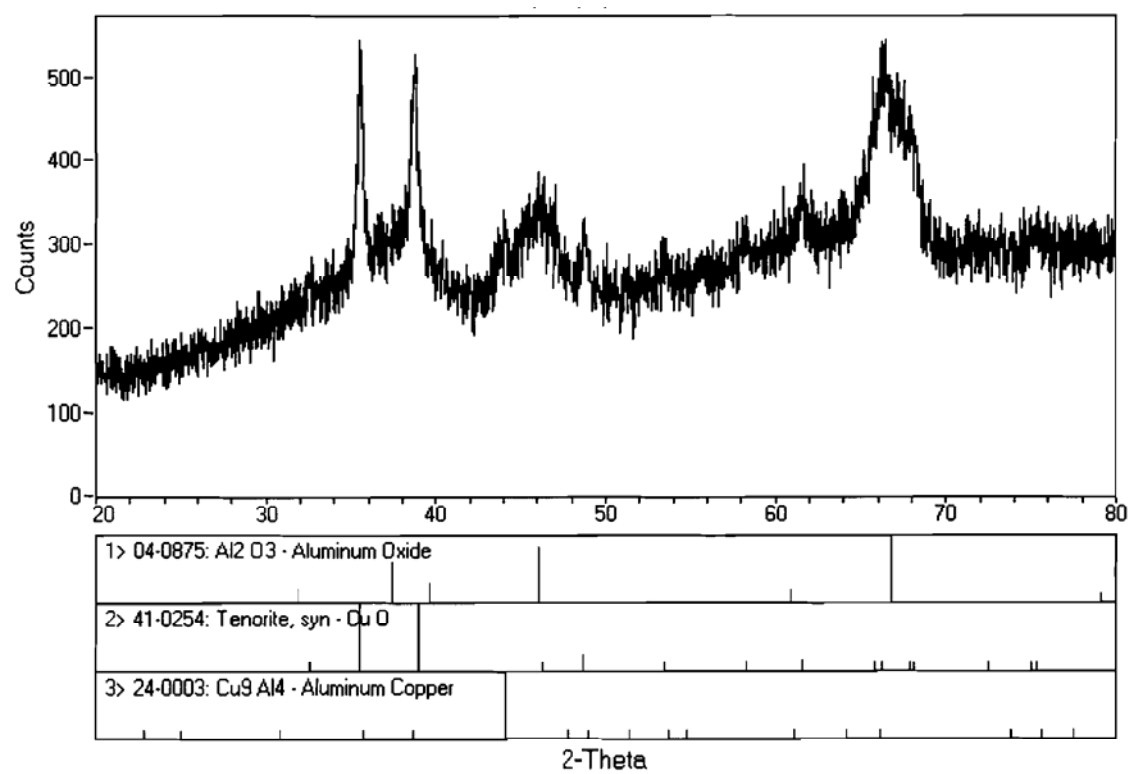


**Figure 3.3:** XRD spectrum of 20 wt% Cu/alumina

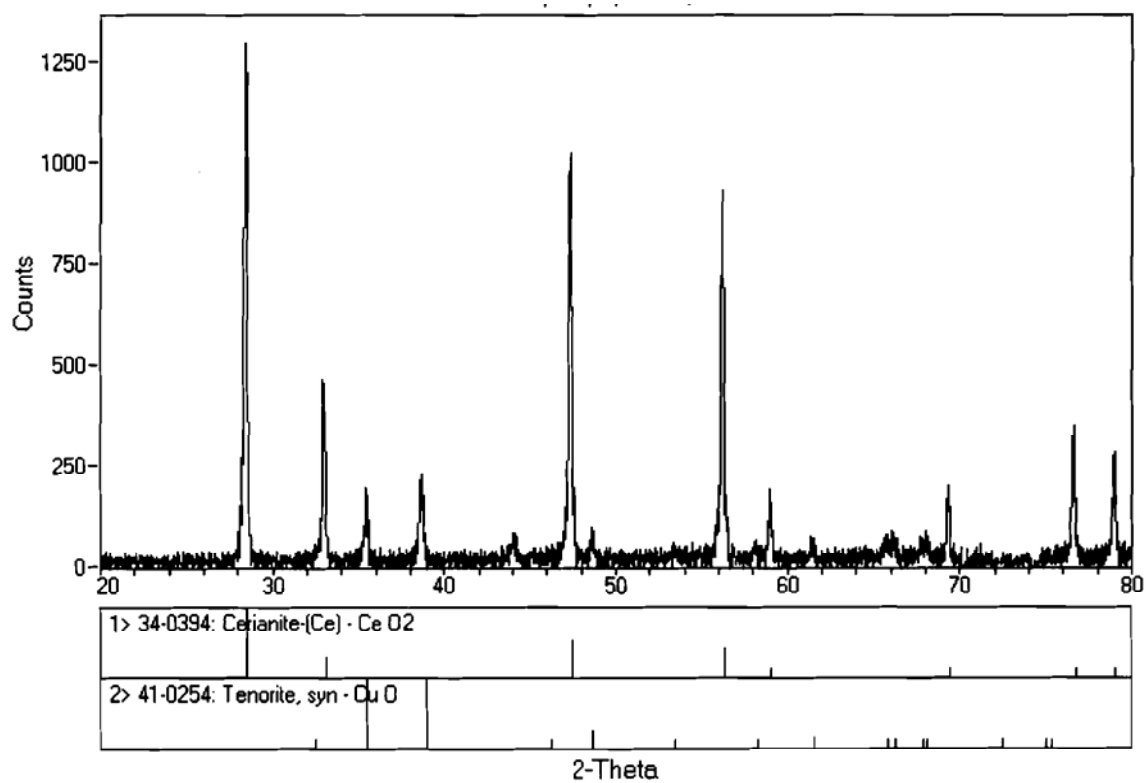
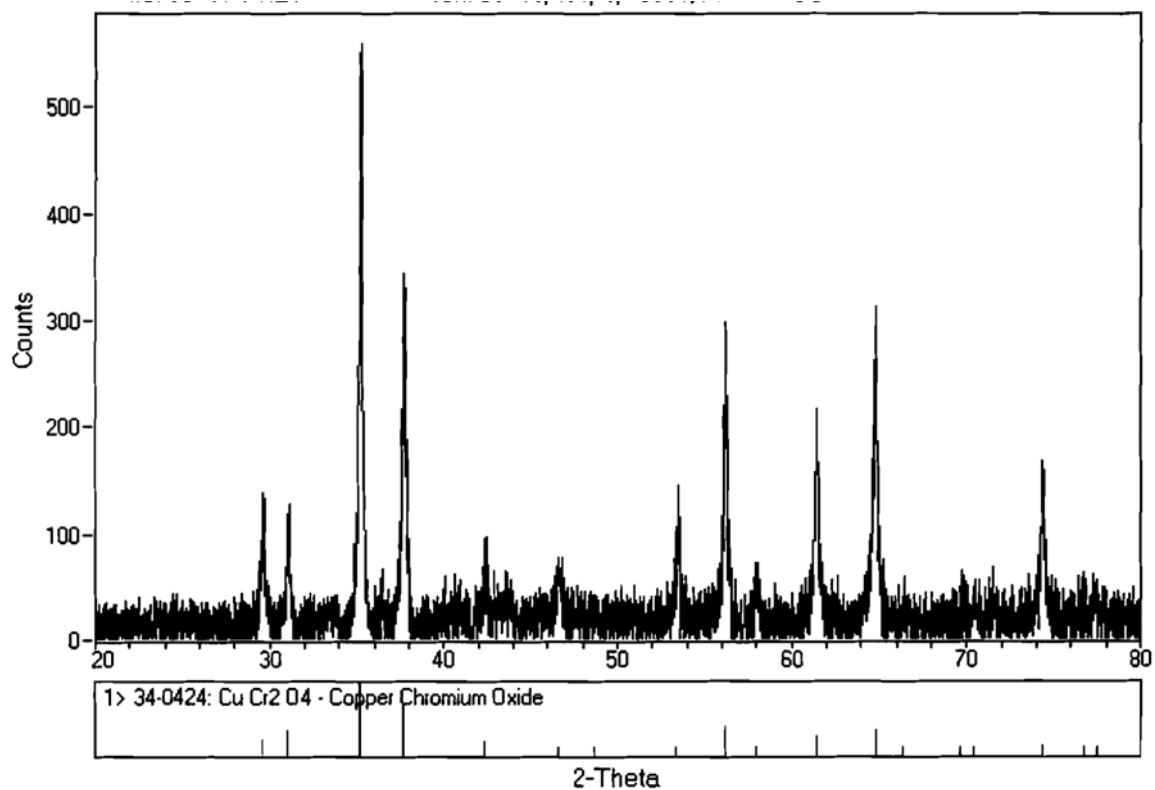


**Figure 3.4:** XRD spectra of Cu-Cr-O (Top) and Cu-Ce-O (Bottom) binary oxides

## Chapter 4

### Preliminary Evaluation of Sorbents

#### 4.1 Introduction

Synthesized sorbents were evaluated for Hg-sorption in N<sub>2</sub> atmosphere over the temperature range 423–533 K. The purpose of these screening tests was to identify reactive metal oxides for detailed evaluation in simulated fuel gas conditions.

#### 4.2 Experimental Methods

##### *Experimental Setup*

The sorbents were evaluated in a lab-scale, fixed bed reactor with the outlet mercury concentration monitored by a semi-continuous mercury analyzer. As shown in Figure 2.1, the mercury sorbent testing unit essentially consists of a quartz reactor shell and a quartz reactor insert that are externally heated by a three-zone electric furnace. The setup is complete with equipment for feeding and measuring the flow rate of the gases, measuring and controlling the bed temperature, monitoring the reactor pressure and the pressure drop across the bed, off-gas sampling and analysis, and an automated data acquisition system. The reactor system is configured for upward gas flow, and the three-zone furnace is positioned with respect to the sorbent bed to accomplish feed gas preheating. Certified elemental mercury (Hg<sup>0</sup>) permeation tube from VICI Metronics is used to generate the Hg<sup>0</sup> vapor. The permeation tube is housed in a VICI Metronics U-tube, heated in a constant temperature water bath. The reactor insert has a 2.3 cm O.D. and a 1.8 cm I.D. sorbent bed cage of a 1 cm height. The top of the cage is a fixed porous frit, while the bottom consists of a similar, but removable porous frit to allow for placement of the sorbent. The height of the sorbent bed is maintained around 0.5 cm, with the bed sandwiched between quartz wool packing. A “semi-continuous” gas-phase mercury analyzer (PSA Sir Galahad II) is used to monitor the concentration and speciation of mercury in the gas stream.

##### *Experimental Procedure*

Approximately 0.2 g of the sorbent (size range 180–250 μm) was mixed with 1.8 g of inert alumina (size range 250–425 μm) to prevent channeling of mercury within the sorbent bed. The sorbent was loaded in the quartz reactor insert and the sorbent bed was supported by quartz wool and porous frit on both sides. Next, the reactor was inserted in the shell and preheated to the desired temperature in flowing 2.6 lpm of N<sub>2</sub> stream. A mercury permeation tube was used as a source of mercury with 0.4 lpm N<sub>2</sub> used as a mercury carrier stream. When the temperature, flow rate, and bypass mercury concentration values were stabilized, the mercury was sent to the sorbent, and the outlet concentration (including mercury speciation) was monitored and recorded by the PSA analyzer. The mercury loading on the sorbent was calculated based on the area above the breakthrough curve. For selected experiments, this result was confirmed using a DMA-80 Direct Mercury Analyzer from Milestone, Inc., which measured total mercury loaded on the sorbent.

##### *Presulfidation of Sorbents*

To evaluate Hg capture by nanocrystalline metal sulfides, NanoActive CuO and MnO<sub>2</sub> sorbents were presulfided in the presence of 0.5 slpm of 10% H<sub>2</sub>S/N<sub>2</sub> stream for 3 h. The sulfidation of NanoActive CuO and MnO<sub>2</sub> was carried out at 423 K and 573 K, respectively.

### 4.3 Results and Discussion

#### *Evaluation of NanoActive Sorbents for Mercury Capture*

Mercury sorption capacities of the eight NanoActive metal oxides were determined by following the procedure given earlier. The sorption studies were carried out at two different temperatures of 423 and 533 K with 3 slpm of Hg-laden N<sub>2</sub> stream. The inlet mercury concentration varied over the range of 125–140 µg/m<sup>3</sup> for these experiments, believed to be due to the day-to-day variation of the analyzer calibration.

NanoActive TiO<sub>2</sub>, CeO<sub>2</sub>, ZnO and MoO<sub>3</sub> sorbents were ineffective in capturing mercury, and their Hg-sorption capacities were negligible at both the temperatures. Table 4.1 gives a summary of the results for the NanoActive CuO, MnO<sub>2</sub>, MnO<sub>2</sub>/alumina, and Cr<sub>2</sub>O<sub>3</sub> sorbents. It should be noted that the Hg-sorption capacity given in the table represents the sorbent capacity for the duration for which the sorbent was exposed to mercury, and not the saturation sorption capacity. In this table, the total mercury captured as a percentage is calculated by dividing the total mercury captured by the sorbent by the total mercury exposed to the sorbent.

Of the eight nanocrystalline sorbents evaluated in this work, NanoActive Cr<sub>2</sub>O<sub>3</sub> was the most effective at both the temperatures. Increasing the NanoActive MnO<sub>2</sub> sorbent surface area by supporting it on a high surface area alumina increased the Hg-sorption capacity of the sorbent, which suggest that the sorption of Hg takes primarily at the surface. Although the Hg-capacities of NanoActive Cr<sub>2</sub>O<sub>3</sub> and MnO<sub>2</sub>/alumina are similar, the surface area of the latter is more than twice that of the former (240 vs. 103 m<sup>2</sup>/g). Since Hg-sorption is a surface phenomenon, Hg-sorption capacities should be compared based on the sorbent surface area. Therefore, it can be concluded that the Hg-sorption capacity of Cr<sub>2</sub>O<sub>3</sub> is higher than that of MnO<sub>2</sub>. Figure 4.1 shows a typical Hg breakthrough plot for NanoActive MnO<sub>2</sub>/alumina sorbent at 423 K.

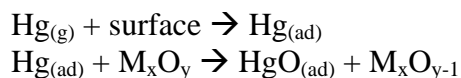
#### *Mechanism of Mercury Capture by Sorbents*

Results in Table 4.1 indicate that mercury-sorption capacity of the sorbents decrease at higher temperature, suggesting that physical adsorption is the controlling mechanism of mercury capture. As outlined below, further studies were carried out to understand the mechanism of interaction between mercury and the sorbents.

NanoActive MnO<sub>2</sub> Sorbent: To further confirm the physical adsorption mechanism for NanoActive MnO<sub>2</sub> sorbent, an experiment was carried out in which the sorbent, after exposure to the mercury stream, was exposed to mercury-free N<sub>2</sub> stream. Figure 4.2 shows the adsorption and desorption cycle for NanoActive MnO<sub>2</sub> sorbent. In this experiment, approx. 0.1 gm of the sorbent was mixed with 1.9 gm of inert alumina and exposed to 115 µg/m<sup>3</sup> of Hg/N<sub>2</sub> stream at 423 K. After 1 h of exposure, the mercury stream was diverted to the vent and only N<sub>2</sub> was passed over the sorbent. At approx. 2.75 h into the desorption stage, temperature of the sorbent was increased to 468 K. This temperature increase resulted in further release of adsorbed mercury from the sorbent. The amount of Hg released by sorbent in the N<sub>2</sub> stream was recorded by the PSA mercury analyzer. Calculations indicate that about 16 µg of Hg was captured by the sorbent during adsorption, whereas, only 3.6 µg of total Hg was released during desorption. Therefore, it is concluded that Hg is adsorbed on the sorbent surface by physical (weak van der Waal's forces) as well as strong chemical forces, and a much higher temperature is required for its complete release from the sorbent surface.

NanoActive Cr<sub>2</sub>O<sub>3</sub> sorbent: Adsorption/desorption studies were also carried out for NanoActive Cr<sub>2</sub>O<sub>3</sub> sorbent. As shown in Figure 4.3, after Hg adsorption for 1 h at 423 K in N<sub>2</sub>, the sorbent temperature was gradually increased to 443, 473, and 523 K in Hg-free N<sub>2</sub> stream. The amount of mercury released increased with the desorption temperature. However, of the 22.6 µg of Hg captured during the 1-h adsorption, only 2.7 µg of Hg was released during desorption, suggesting that the balance Hg is captured on the sorbent surface by stronger chemical forces.

An oxidation mechanism has been suggested by Granite et al.<sup>1</sup> for capture of Hg by metal oxide catalysts such as MnO<sub>2</sub> and Cr<sub>2</sub>O<sub>3</sub>. According to the proposed mechanism, in the first step of the capture process, gas phase Hg is physically adsorbed on the sorbent surface, which in the second step is oxidized to HgO by the lattice oxygen of the metal oxide (M<sub>x</sub>O<sub>y</sub>) catalyst. The mechanism can be given as<sup>1</sup>:



During the desorption stage, the physically adsorbed mercury on the surface Hg<sub>(ad)</sub> is released, however, the chemically adsorbed mercury (HgO<sub>(ad)</sub>) remains on the sorbent surface.

NanoActive CuO sorbent: An unusual shape of the breakthrough curve was obtained when mercury was exposed to 0.2 gm of NanoActive CuO sorbent at 423 K (see Figure 4.4). It can be seen that the outlet mercury concentration reached a steady value of approx. 92 µg/m<sup>3</sup> at the end of 30 min exposure to mercury, suggesting that a complete breakthrough could never be obtained. To investigate this further, the experiment was repeated under identical conditions. A similar behavior was observed even for the repeat experiment. It is speculated that the NanoActive CuO sorbent has some catalytic activity that results in oxidation of a certain fraction of incoming elemental mercury. This oxidized mercury is captured by the same sorbent. Since the sorbent remains catalytically active for the duration of the experiment, mercury breakthrough is not observed. To reduce the experimental time so that a complete breakthrough could be observed, an experiment was carried out at 423 K with only 0.05 gm of the sorbent mixed with 1.95 gm of inert alumina. The sorbent achieved near saturation during the 4 h exposure to Hg.

#### *Mercury Sorption on Presulfided Sorbents*

Presulfided NanoActive CuO and MnO<sub>2</sub> sorbents were evaluated for Hg capture in N<sub>2</sub> stream at 423 and 533 K following the procedure given earlier. Presulfided NanoActive MnO<sub>2</sub> was not effective at either of the temperatures, whereas, presulfided NanoActive CuO was effective only at 423 K. During the 5-h exposure to mercury, the presulfided NanoActive CuO captured nearly 370 µg Hg/g sorbent, which corresponded to 71% of total exposed mercury. Comparison with the Hg-capacity of NanoActive CuO given in Table 4.1 indicates that sulfided CuO has higher capacity and efficiency for Hg capture. The increased capacity of the sulfided sorbent is due to the formation of CuS during presulfidation, which has increased affinity towards Hg.

## **4.4 Conclusions**

Preliminary evaluation of nanocrystalline metal oxide and sulfide sorbents was carried out in N<sub>2</sub> stream to screen effective mercury sorbents for further evaluation in simulated fuel gas. Of the eight sorbents evaluated in this work, NanoActive Cr<sub>2</sub>O<sub>3</sub> was the most effective at 423 and 533 K. NanoActive MnO<sub>2</sub> and CuO sorbents also showed promise in capturing Hg from N<sub>2</sub> stream. Mechanistic studies suggested that Hg was captured on the sorbent surface by a combination of

physical and chemical sorption mechanisms. Sulfidation of NanoActive CuO sorbent increased its Hg-sorption capacity at 423 K, however, the sulfided CuO was not effective at 533 K.

### **Literature Cited**

1. Granite E.J., H.W. Pennline, and R.A. Hargis, Novel sorbents for mercury removal from flue gas, *Ind. Eng. Chem. Res.*, **39**(4), 1020–1029, 2000.

**Table 4.1:** Comparison of Hg-sorption capacities of NanoActive® sorbents

	423 K				533 K			
	CuO	MnO <sub>2</sub>	MnO <sub>2</sub> /alumina	Cr <sub>2</sub> O <sub>3</sub>	CuO	MnO <sub>2</sub>	MnO <sub>2</sub> /alumina	Cr <sub>2</sub> O <sub>3</sub>
Inlet Hg conc., $\mu\text{g}/\text{m}^3$	130	125	138	130	140	132	135	133
Final outlet Hg conc., $\mu\text{g}/\text{m}^3$	97	45	10	4	140	106	75	56
Sorption time, h	6	6	4	6	2.5	5	6	6
Hg-sorption capacity, $\mu\text{g}/\text{g}$	250	490	480	720	74	230	500	530
Total Hg captured, %	36	73	97	~100	21	32	70	73



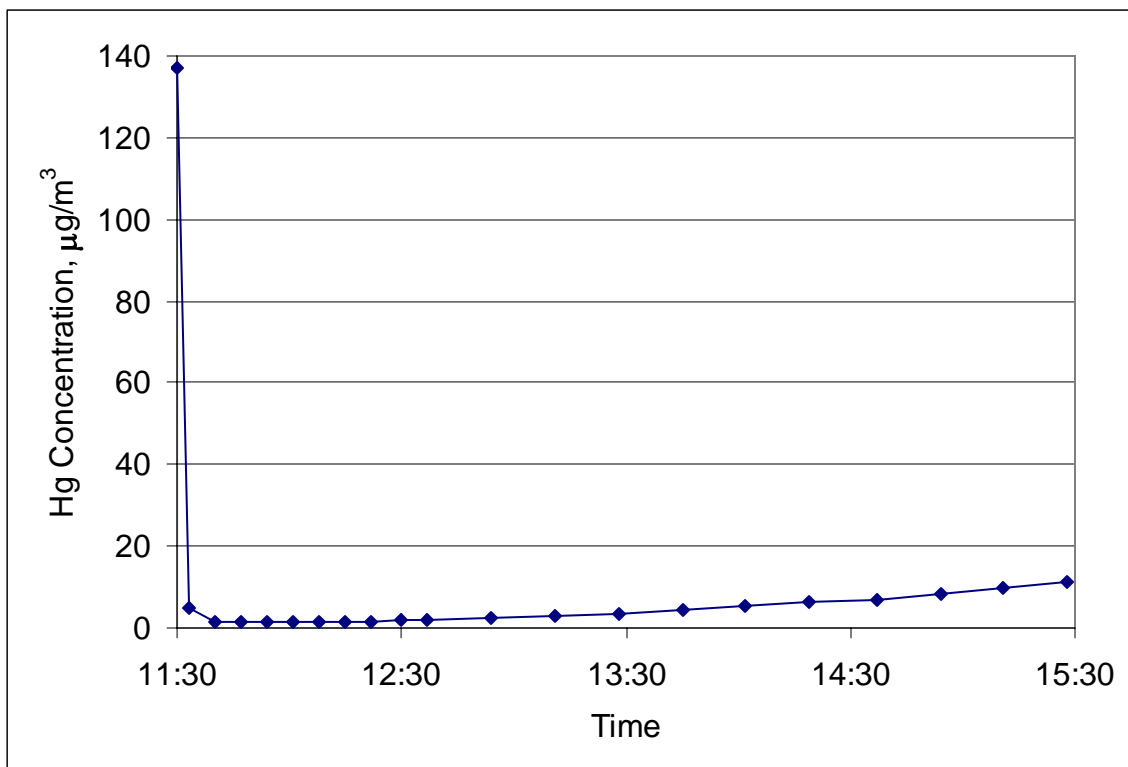


**Figure 4.1:** Mercury breakthrough plot for NanoActive MnO<sub>2</sub>/alumina sorbent at 423 K

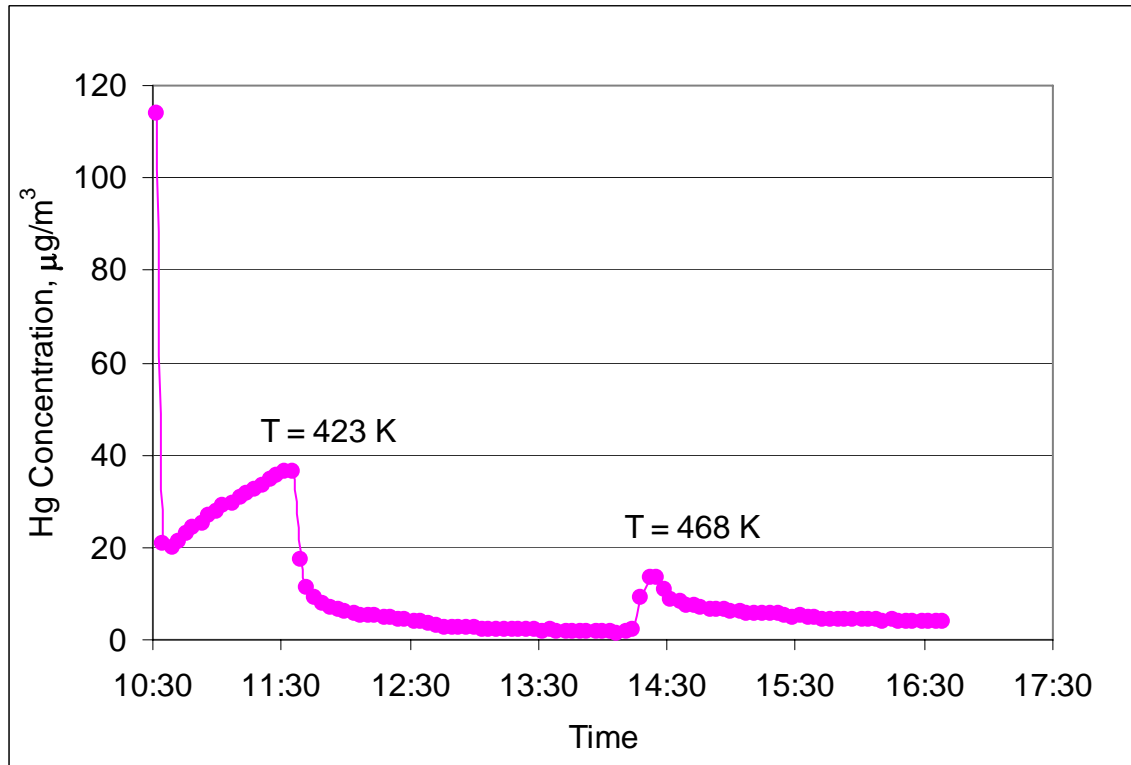


**Figure 4.2:** Adsorption/desorption studies on NanoActive MnO<sub>2</sub> sorbent

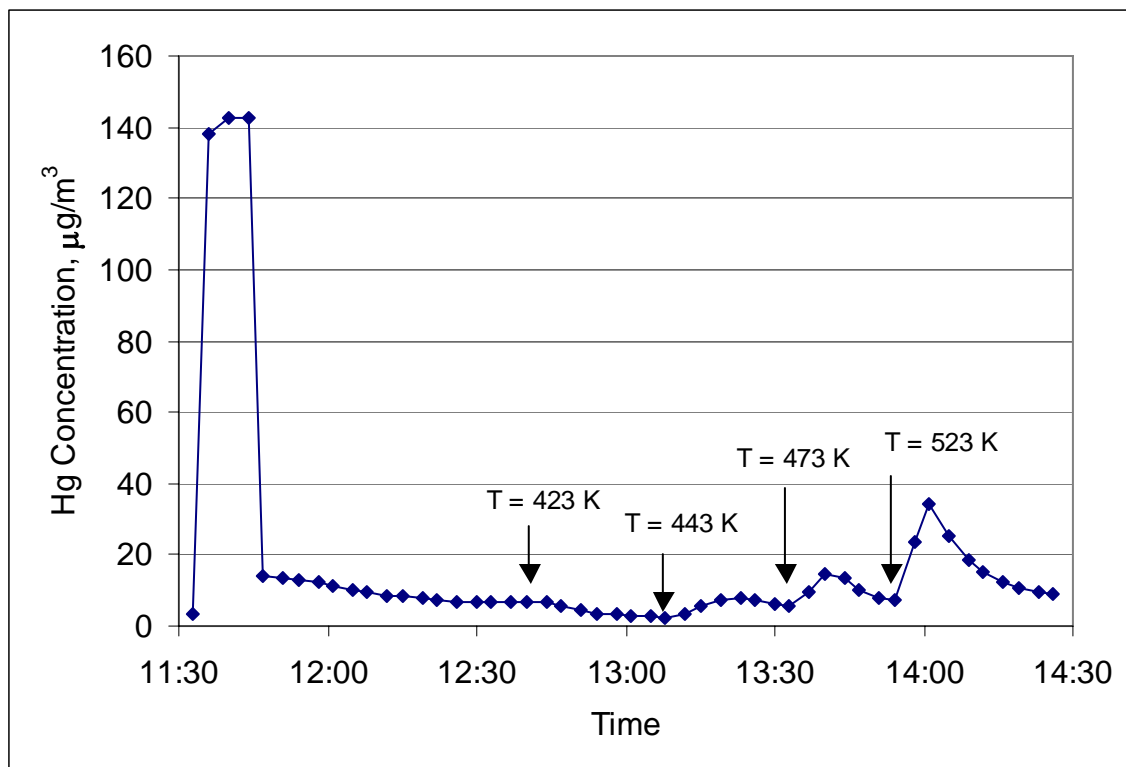


**Figure 4.3:** Adsorption/desorption studies on NanoActive  $\text{Cr}_2\text{O}_3$  sorbent

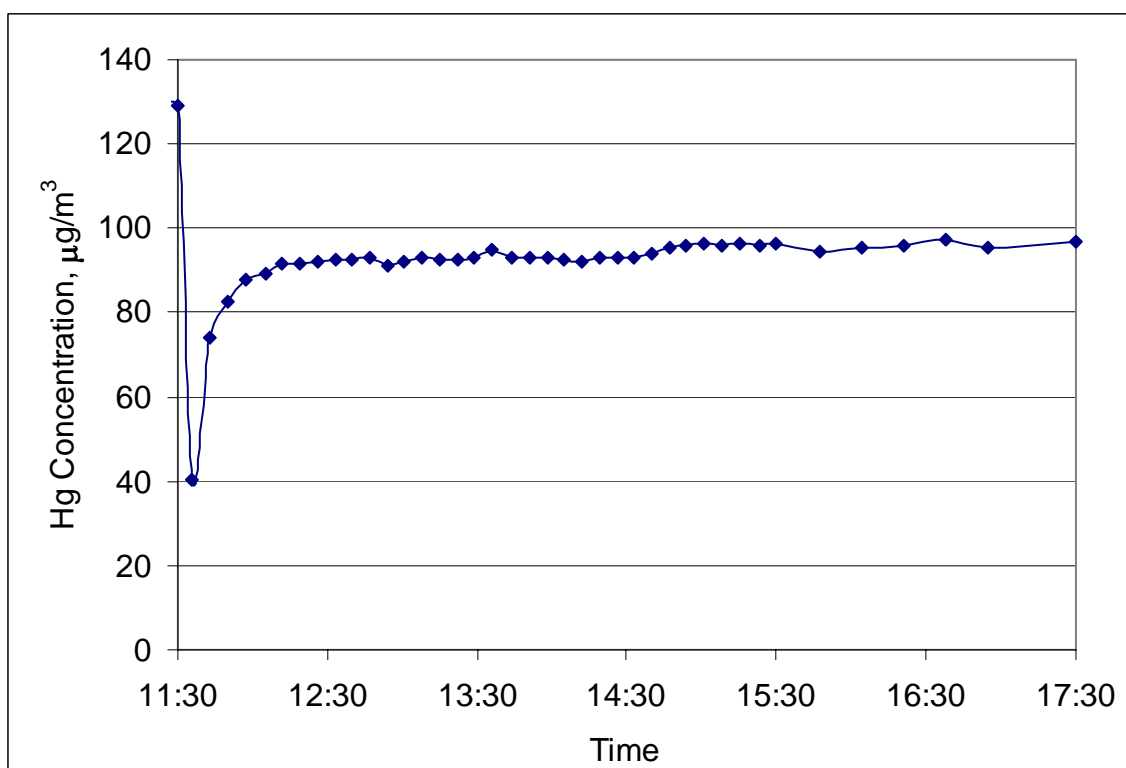


**Figure 4.4:** Mercury breakthrough plot for NanoActive  $\text{CuO}$  at 423 K

## Chapter 5

### Sorbent Evaluation in Simulated Fuel Gas

#### 5.1 Introduction

Results of the sorbent screening tests in N<sub>2</sub> atmosphere detailed in Chapter 4 suggested that NanoActive CuO, MnO<sub>2</sub>, and Cr<sub>2</sub>O<sub>3</sub> were the most reactive sorbents. However, when pre-sulfided, NanoActive CuO was the most effective of these in N<sub>2</sub> atmosphere. Therefore, CuO was selected for detailed studies in simulated fuel gas (SFG) atmosphere. Several Cu-based sorbents were synthesized and evaluated for capture of mercury (Hg) in SFG atmosphere at temperatures in the range 423–533 K. Nanocrystalline sorbents prepared by NanoScale Materials, Inc. (NanoScale) as well as in-house (GTI) sorbents were evaluated. Copper was supported on high-surface area materials (such as alumina) to increase the total surface area of the sorbent. Details of the synthesis procedure and the properties of supported Cu-based sorbents are given in Chapter 3.

#### 5.2 Experimental Methods

##### *Evaluation of Supported Cu/alumina Sorbents*

The supported Cu-based sorbents were evaluated for Hg-sorption capacity in GTI's mercury sorbent testing system. Initial screening tests were carried out in H<sub>2</sub> and H<sub>2</sub>S containing gas stream with composition (mol %): H<sub>2</sub>/H<sub>2</sub>S/N<sub>2</sub> = 25/0.125/balance. Hydrogen was added to simulate the effect of reducing species, whereas, H<sub>2</sub>S was added to simulate the effect of S-containing species in the gasifier fuel gas. Selected sorbents were evaluated in SFG with the composition (mol %): H<sub>2</sub>/CO/CO<sub>2</sub>/H<sub>2</sub>O/H<sub>2</sub>S/COS/N<sub>2</sub> = 30/30/10/20/0.4/0.04/balance. The total flow rate of the gas was maintained at 2 slpm, whereas, the concentration of Hg in the gas stream was around 180 µg/m<sup>3</sup>. To simulate the effect of high-pressure gasifier conditions, for selected tests, the concentration of Hg was maintained at 2500 µg/m<sup>3</sup>. The sorption of mercury was carried out at temperatures over the range 423–533 K. Unless otherwise noted, about 0.5 g of the sorbent and 225,000 h<sup>-1</sup> (STP) gas hourly space velocity (GHSV) was used.

##### *Mechanism of Hg-sorption by Supported Sorbents in SFG*

To understand the nature of Hg capture mechanism by the supported sorbent, post-sorbed sorbent was exposed to Hg-free gas stream and the desorbed amount of Hg was analyzed by the analyzer. About 0.5 g of the sorbent (20 wt% Cu/alumina) was loaded in a quartz reactor enclosed in an electric furnace maintained at 423 K. Initially, the sorbent was pre-reduced in the presence of 2% H<sub>2</sub>/N<sub>2</sub> to obtain the reduced form of the sorbent. The sorbent was next sulfided for 1 h in a SFG with the composition given above. The flow rate of the gas was maintained at 2 slpm. After sulfidation, about 180 µg/m<sup>3</sup> of mercury was added to the fuel gas stream and the outlet mercury concentration was monitored with a mercury analyzer. The adsorption reaction was carried out for about 90 min, after which the sorbent was desorbed in 2 slpm of N<sub>2</sub> stream at 423 K followed by desorption in Hg-free SFG stream at the same temperature. The amount of Hg captured during adsorption and released during desorption was calculated from the breakthrough curves.

##### *Multicyclic Studies on NanoActive Sorbent*

To evaluate the multicycle potential of nanocrystalline sorbents for Hg capture, the post-sorption sorbent was regenerated in Hg-free stream and again exposed to Hg/SFG stream to undergo the

next capture cycle. Because of the time limitation, only two adsorption/regeneration cycles were carried out. The experimental conditions for the adsorption were the same as given above. The sorbent regeneration was carried out at 473 K in a SFG that was free of Hg, H<sub>2</sub>S and COS.

### 5.3 Results and Discussion

#### *Evaluation of Supported Cu/alumina Sorbents*

GTI's Sorbent: A 20 wt% Cu/alumina sorbent, prepared at GTI, was evaluated for mercury sorption capacity at 473 K. The gas composition was (mol %): H<sub>2</sub>/H<sub>2</sub>S/N<sub>2</sub> = 25/0.125/balance. As seen from Figure 5.1, the sorbent maintains a very high efficiency for Hg capture for 4 h, capturing nearly 100% of incoming mercury. The amount of mercury captured by sorbent during 4 h exposure is calculated as 170 µg/g. The trend of the breakthrough plot suggests that the sorbent has a potential to achieve much higher Hg-sorption capacity while removing more than 90% of incoming Hg. The high capacity of the sorbent is believed to be a result of its high surface area. The 20 wt% Cu/alumina sorbent was also evaluated at 533 K under similar conditions. However, the sorbent did not show much affinity for Hg at this temperature. Possible sorbent deactivation due to carbon formation in the reactor from CO was suspected. Comparison of the results at 423 and 533 K suggests that mercury capture by the sorbent is dominated by physical adsorption mechanism.

NanoActive Cu-based sorbents: A NanoActive 5 wt% CuO/alumina sorbent was evaluated for Hg capture at 473 K in a gas containing H<sub>2</sub>/H<sub>2</sub>S/N<sub>2</sub> with the composition given earlier. As seen from Figure 5.2, the NanoActive sorbent captured nearly 100% of incoming mercury and achieved a high capacity of approx. 170 µg/g in 4 h.

The same nanocrystalline sorbent, when evaluated at 533 K, gave small capacity of mercury (see Figure 5.3). Although the Hg-sorption capacity is lower as compared to 473 K, the sorbent can still remove moderate amount of mercury at the higher temperature of 533 K. The lower capacity at higher temperature suggests physical adsorption as the dominant mercury-capture mechanism.

Since the nanocrystalline sorbent was more effective at lower temperature, it was evaluated at 423 K in SFG of composition: H<sub>2</sub>/CO/CO<sub>2</sub>/H<sub>2</sub>O/H<sub>2</sub>S/COS/N<sub>2</sub> = 30/30/10/20/0.4/0.04/balance (%). In addition, to simulate the effect of high-pressure syngas, the concentration of mercury in the SFG was maintained at 2500 µg/m<sup>3</sup>. For this experiment, 0.75 g of the sorbent was used and the gas hourly space velocity GHSV was maintained at 150,000 h<sup>-1</sup> (STP). Figure 5.4 shows the breakthrough curve of mercury capture by the nanocrystalline sorbent. During the 5-h exposure, the sorbent captured nearly 100% of incoming mercury. The Hg-sorption capacity of the sorbent is calculated as 2 mg/g (0.2 wt%). Based on the trend of the breakthrough curve, it appears that the nanocrystalline sorbent has a potential to achieve much higher Hg-sorption capacity while removing 100% of incoming mercury at 423 K. Such a high Hg-sorption capacity of the sorbent is believed to be due to its high surface area and small crystallite size.

#### *Mechanism of Hg-sorption by Supported Sorbents in SFG*

As described earlier, to understand the mechanism of Hg sorption, the 20 wt% Cu/alumina sorbent (prepared in-house) was exposed to different gases under different conditions and the outlet Hg concentration monitored. Figure 5.5 shows the concentration of Hg at the bed exit under different conditions. At point A, adsorption is started by sending Hg to the reactor. After approx. 90 min, at point B, mercury flow to the sorbent is stopped and the sorbent is exposed to 2

slpm of N<sub>2</sub> at 423 K. It is seen that the amount of mercury released from the sorbent in N<sub>2</sub> is very low. At point C, the desorbing gas is changed to 2 slpm of 20% H<sub>2</sub>, 30% CO, 8% CO<sub>2</sub>, and balance N<sub>2</sub>. It can be seen that after the introduction of H<sub>2</sub> and CO, the amount of mercury released from the sorbent is greatly increased. Around 150 min into the experiment, as can be seen from the figure, the concentration of released Hg went beyond the analyzer range. At point D, about 0.4% H<sub>2</sub>S and 0.04% COS is added to the gas stream maintaining the total flow at 2 slpm. After the introduction of H<sub>2</sub>S, the release of Hg from the sorbent is suppressed, which suggests that H<sub>2</sub>S and/or COS has a positive effect on the capture of mercury by the supported Cu sorbent. Based on the breakthrough data, it was calculated that about 58 µg/g of Hg was captured by the sorbent during the adsorption stage, and the same amount was released during the desorption stage.

An experiment was also carried out to determine the form of Cu in the spent sorbent. About 0.75 g of 20 wt% Cu/alumina was exposed to 0.125% H<sub>2</sub>S, 25% H<sub>2</sub>, balance N<sub>2</sub> at 473 K for 6 h. X-ray diffractogram (XRD) of the post-reaction sample is shown in Figure 5.6. The figure shows that supported Cu sorbent, when exposed to a gas stream containing H<sub>2</sub>S and H<sub>2</sub>, is converted into CuS and not the thermodynamically favored form Cu<sub>2</sub>S.

Based on these results, the following mechanism of Hg capture by the supported Cu-based sorbents is proposed. When the Cu atoms are dispersed, as is the case with supported sorbents, the distance between two Cu atoms is more than that required to form Cu<sub>2</sub>S compound. Due to this structural restriction, when a supported Cu sorbent is exposed to H<sub>2</sub>S and H<sub>2</sub>, the thermodynamically favored Cu<sub>2</sub>S compound is not formed. Instead, the more reactive CuS is formed on the surface of the support. When the sorbent is exposed to mercury, it forms a bond with the S atom of CuS. This Hg—S bond is broken when the sorbent is desorbed in a gas stream containing H<sub>2</sub> and/or CO, thus releasing Hg from the sorbent.

#### *Multicyclic Studies on NanoActive Sorbent*

Figure 5.7 shows the multicyclic behavior of NanoActive 5wt% CuO/alumina sorbent for Hg capture. It can be seen that the sorption behavior of the sorbent for Hg remains the same for these two cycles. Although only two cyclic studies were carried out, these results demonstrate that the sorbent can be effectively regenerated in SFG stream and used repeatedly for capture of Hg with high efficiency.

#### *Evaluation of Binary Sorbents*

The Hg-sorption capacity of unsupported binary metals oxides (CuO-Cr<sub>2</sub>O<sub>3</sub> and CuO-CeO<sub>2</sub>) was evaluated at 423 K in SFG. However, these sorbents did not have any capacity of Hg at these conditions, probably because of the low surface area of the sorbents (2.2 m<sup>2</sup>/g for CuO-Cr<sub>2</sub>O<sub>3</sub> and 1.2 m<sup>2</sup>/g for CuO-CeO<sub>2</sub>). Since Hg capture by the sorbent is essentially a surface phenomenon, a sorbent with a low surface area would give very low Hg-sorption capacity.

Since unsupported binary metal oxides did not show much affinity for Hg due to the low surface area, binary oxides based on Cu and Cr metals were supported on high surface area alumina to evaluate their effectiveness for Hg capture. Figures 5.8 and 5.9 show the breakthrough plots for 5 wt% Cu/5 wt% Cr/alumina sorbent in H<sub>2</sub>/H<sub>2</sub>S/N<sub>2</sub> stream at 473 and 533 K, respectively. Comparison of these figures indicates that binary metal oxide is more effective at the lower temperature of 473 K, suggesting physical adsorption as the dominant mechanism. The Hg-sorption capacity at 473 K during 4 h exposure is calculated as approx. 150 µg/g.

## 5.4 Conclusions

Several supported Cu-based sorbents were evaluated for capture of Hg in SFG atmosphere at temperatures in the range 423–533 K. Nanocrystalline sorbents prepared by NanoScale as well as in-house sorbents were evaluated. These supported sorbents were found to be effective in capturing Hg at 423 and 473 K. Based on the desorption studies, physical adsorption was found to be the dominant capture mechanism. XRD studies carried out on the post-sorption sorbent suggested that CuS was the chemical form of Cu at 473 K and not the thermodynamically favored Cu<sub>2</sub>S form. Multicyclic studies carried out on a nanocrystalline sorbent demonstrated that the sorbent could be regenerated easily and used over multiple cycles to capture Hg with high efficiency. The experiments demonstrated that H<sub>2</sub>S in the SFG assists in the capture of Hg by forming stable and reactive CuS component. Mercury captured by this CuS is released easily after exposure of the spent sorbent to H<sub>2</sub>-containing stream.

Several formulations of supported and unsupported binary metal Cu-based sorbents were also evaluated for capture of Hg in H<sub>2</sub>S/H<sub>2</sub>/N<sub>2</sub> atmosphere at temperatures 473 and 533 K. At these conditions, supported sorbents showed moderate capacity for Hg capture. The Hg-sorption capacity at 473 K during 4 h exposure is calculated as ca. 150 µg/g. Based on the effect of temperature on capture of Hg by these binary oxide sorbents, physical adsorption was found to be the dominant capture mechanism with lower temperatures favoring capture of Hg.

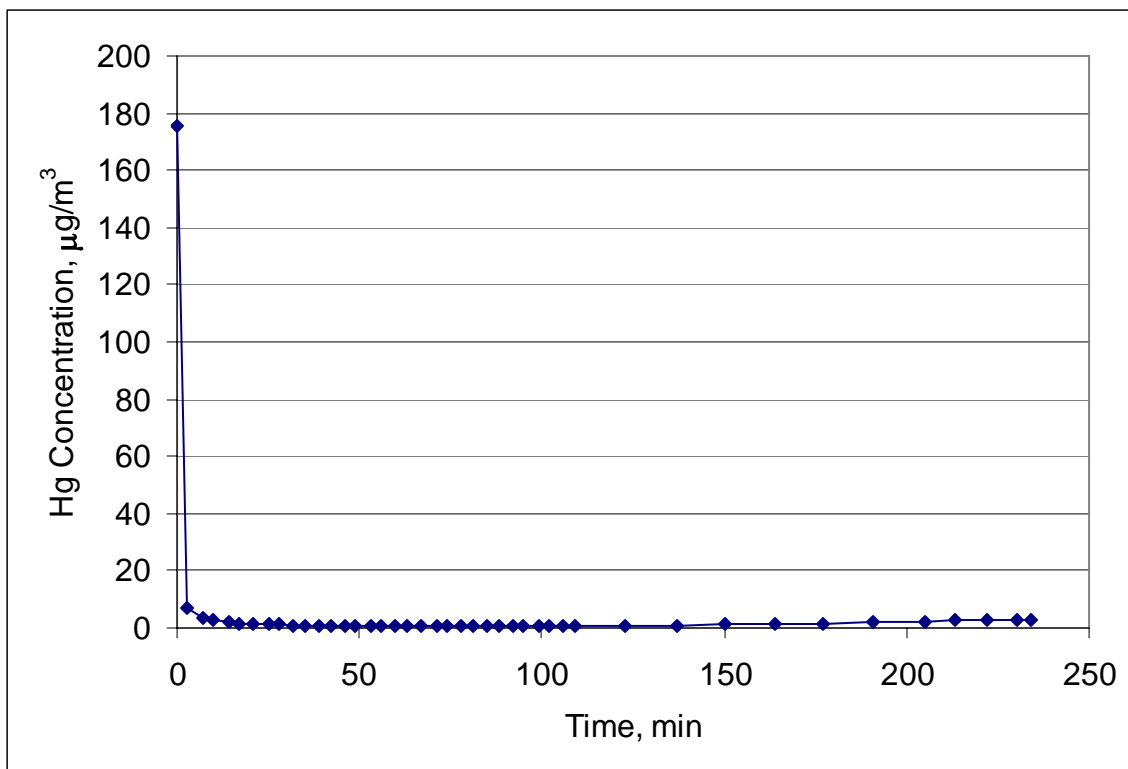


**Figure 5.1:** Mercury breakthrough plot for 20 wt% Cu/alumina sorbent at 473 K

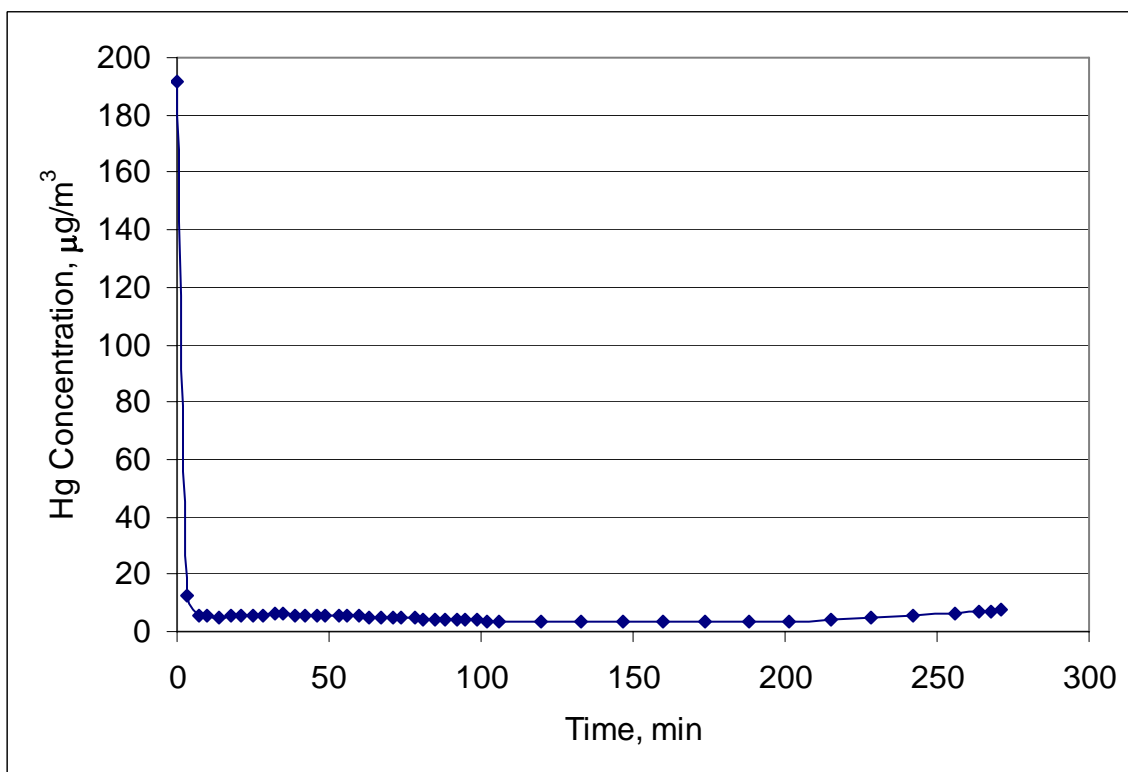


**Figure 5.2:** Mercury breakthrough plot for NanoActive 5 wt% CuO/alumina sorbent at 473 K

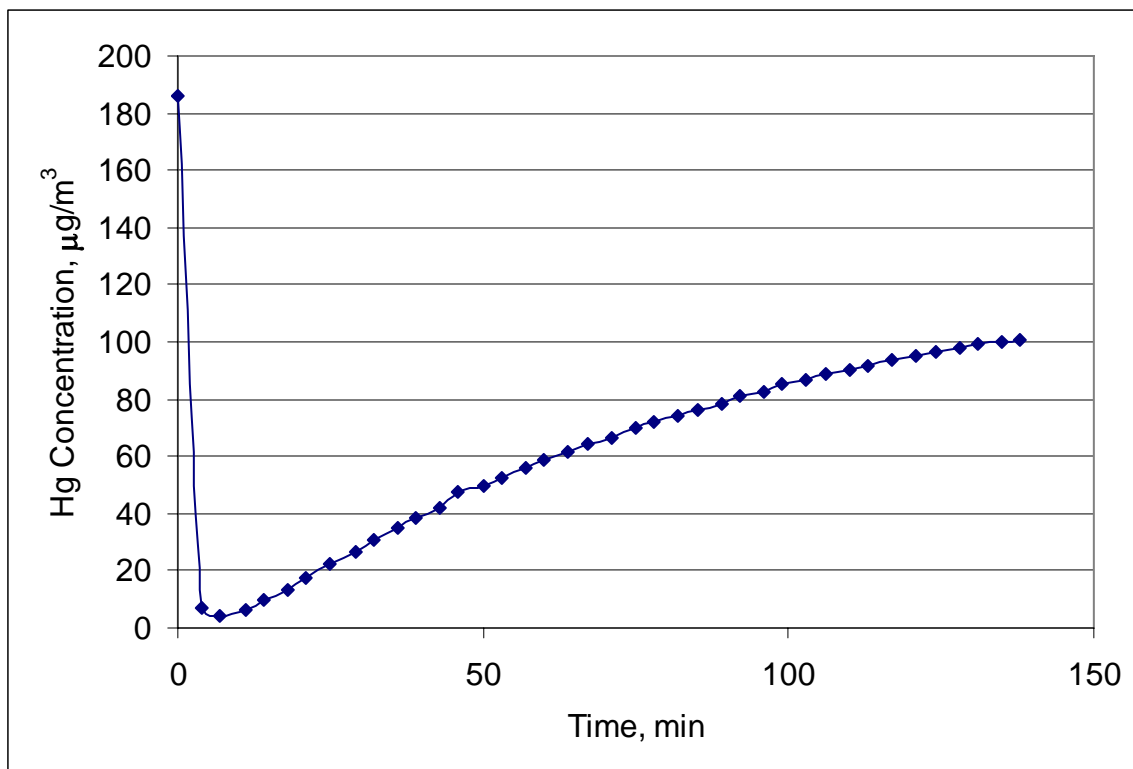


**Figure 5.3:** Mercury breakthrough plot for NanoActive 5 wt% CuO/alumina sorbent at 533 K

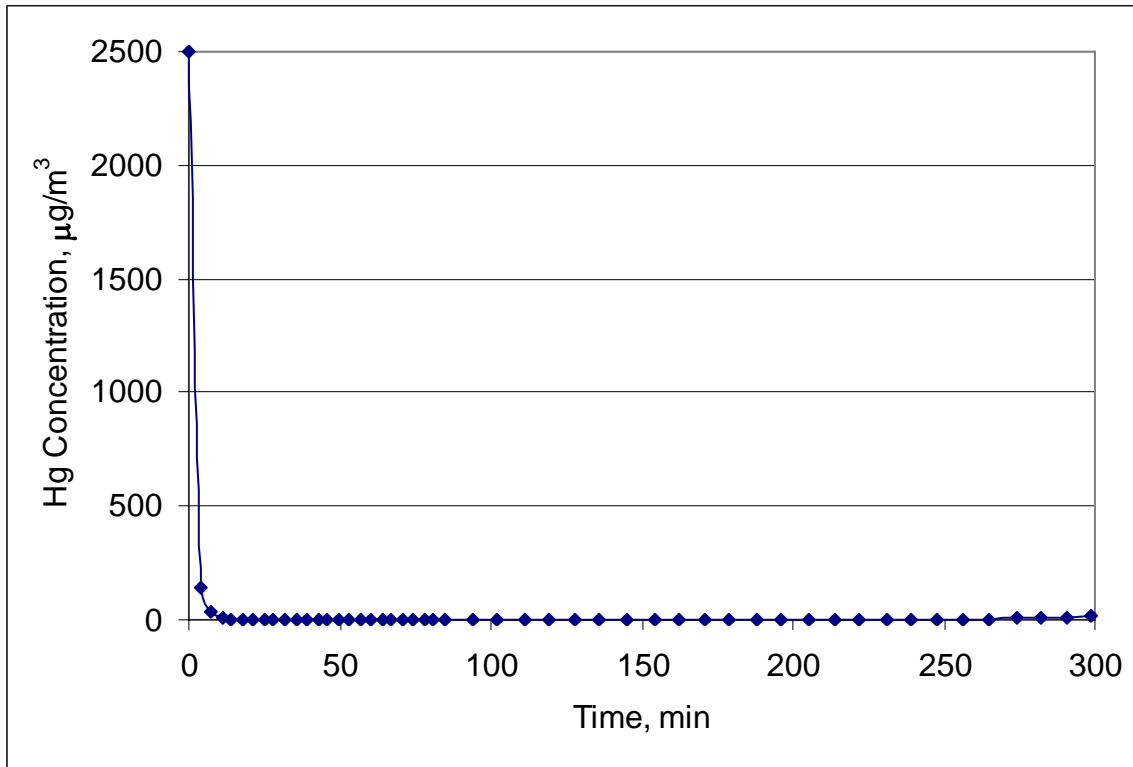


**Figure 5.4:** Mercury breakthrough plot for NanoActive 5 wt% CuO/alumina sorbent at 423 K



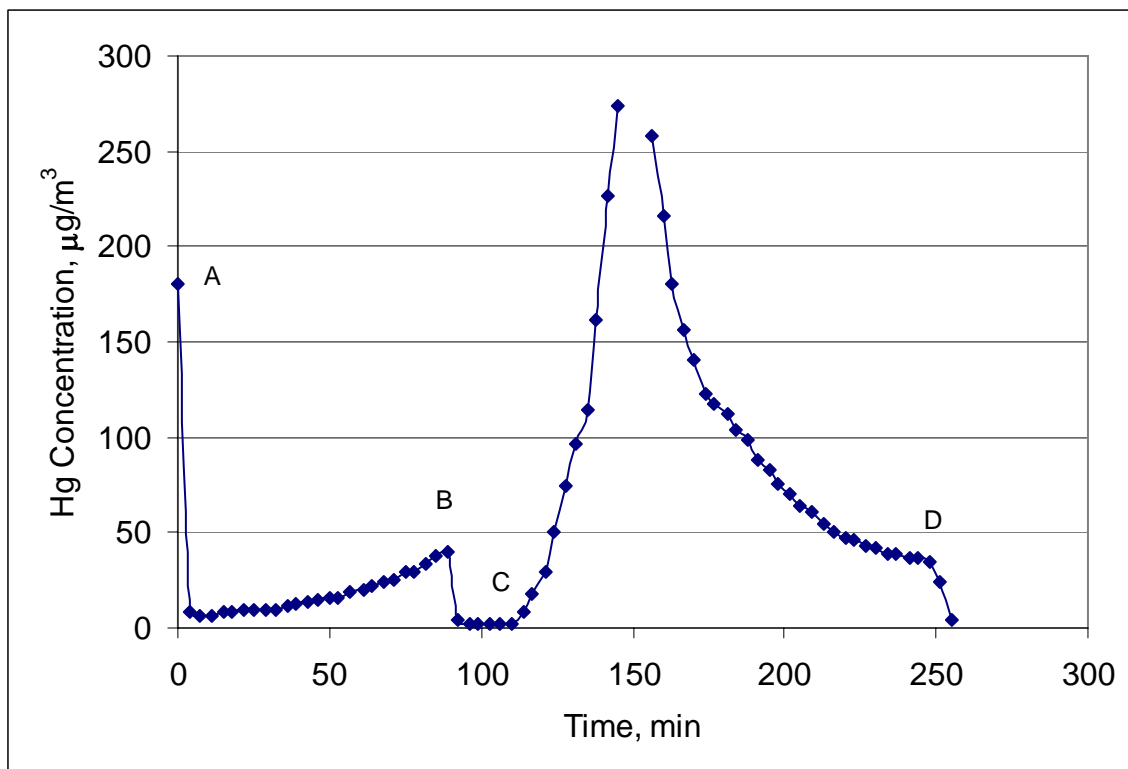


**Figure 5.5:** Adsorption/desorption of Hg on 20 wt% Cu/alumina sorbent at 423 K

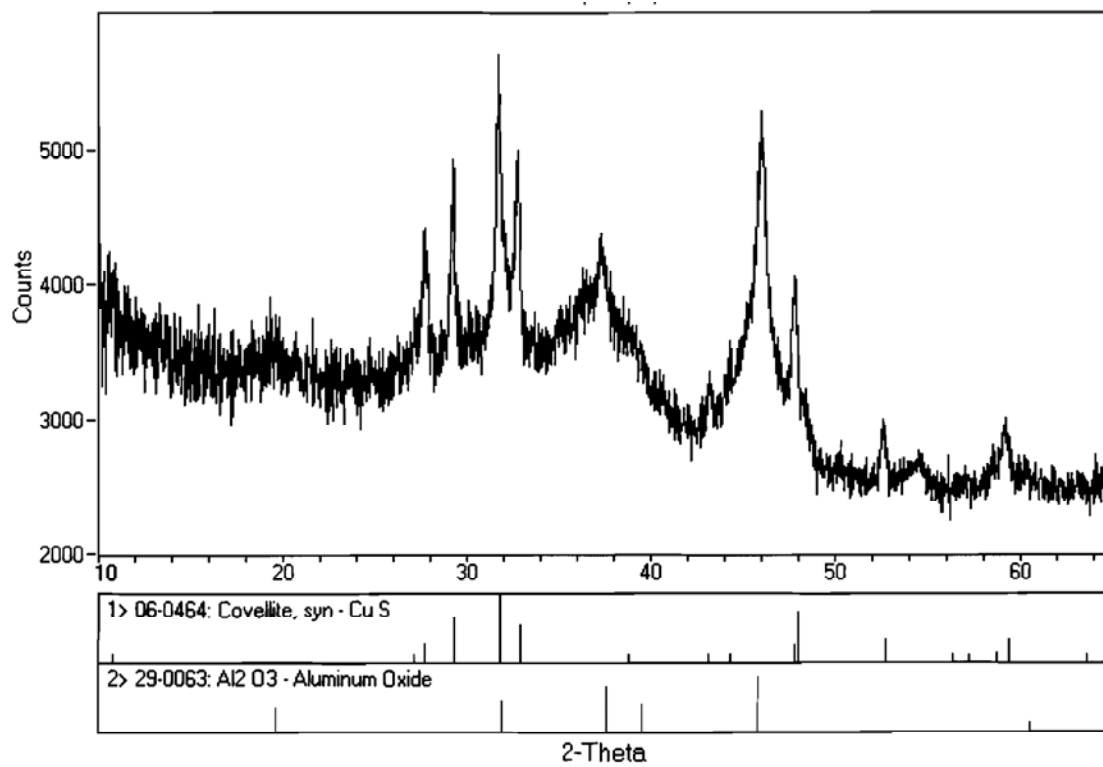


**Figure 5.6:** XRD spectra of 20 wt% Cu/alumina after exposure to H<sub>2</sub>S/H<sub>2</sub>/N<sub>2</sub> stream at 473 K

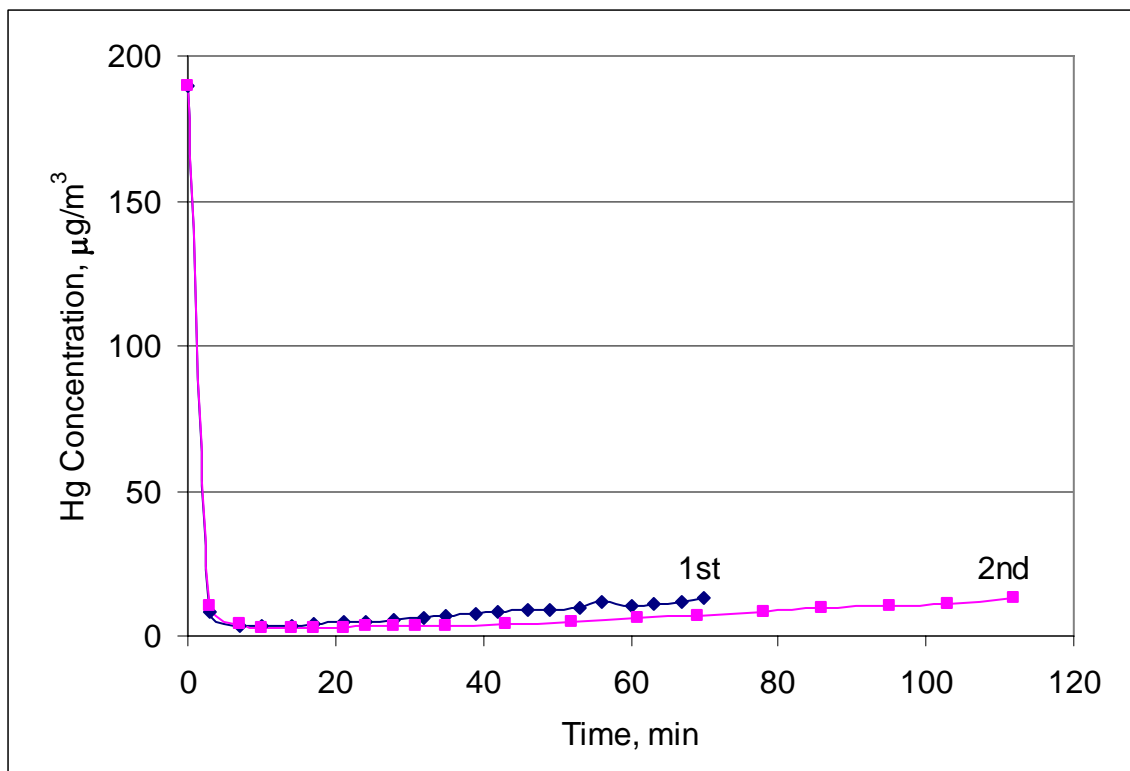


**Figure 5.7:** Multicyclic Hg-sorption studies on NanoActive 5 wt% CuO/alumina

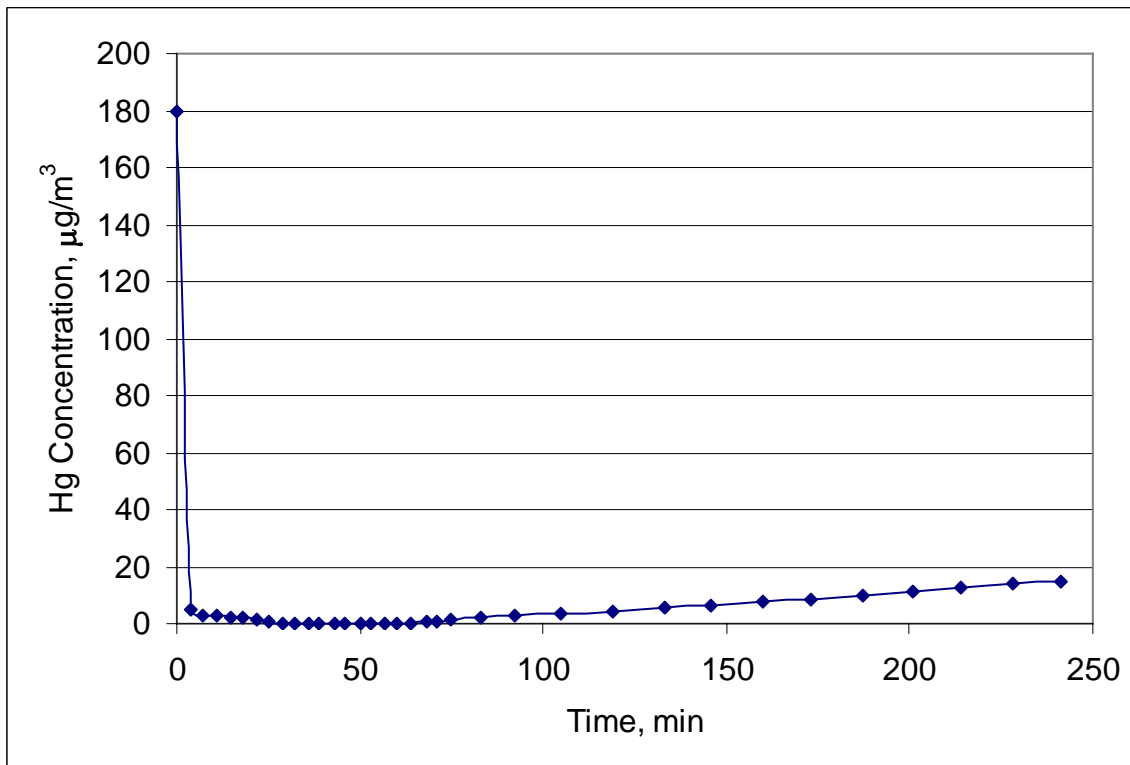


**Figure 5.8:** Mercury breakthrough plot for 5:5 wt% Cu:Cr/alumina sorbent at 473 K

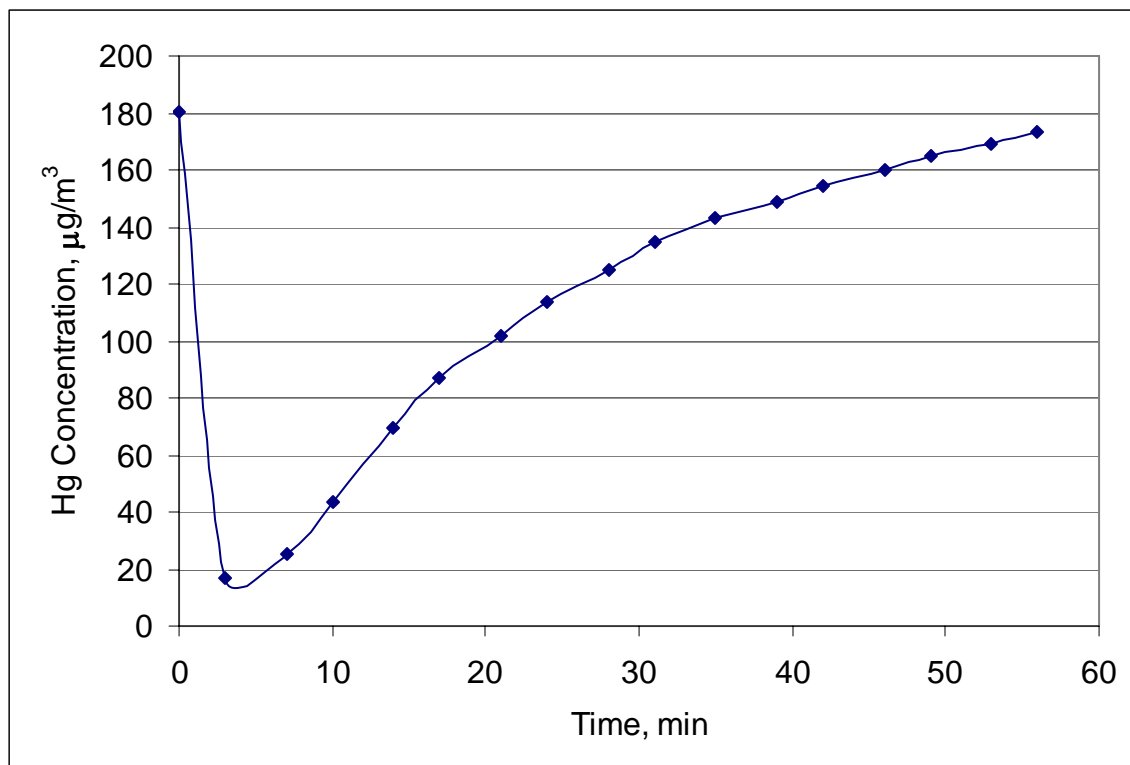


**Figure 5.9:** Mercury breakthrough plot for 5:5 wt% Cu:Cr/alumina sorbent at 533 K

## Chapter 6

### Overall Conclusions

In this project, several different types of metal oxide sorbents were synthesized and evaluated for their potential to capture mercury from high temperature (423–533 K) coal fuel gas. These included nanocrystalline, conventional, mixed-metal oxides and their supported forms. A major focus of the project was on the understanding of the fundamental mechanism responsible for the capture of mercury from simulated fuel gas (SFG).

Initial screening tests in  $N_2$  demonstrated that NanoActive  $Cr_2O_3$  was the most active of the nanocrystalline sorbents evaluated, followed by NanoActive  $MnO_2$  and  $CuO$ . The capture of Hg on these sorbents decreased with temperature, suggesting physical adsorption as the dominating capture mechanism. Detailed desorption studies carried out in Hg-free  $N_2$  stream indicated that some part of captured Hg was attached to the sorbent surface by strong chemical bonds. This “chemisorptive” capture of Hg was the result of oxidation of Hg by the reactive O atoms of the oxides, which resulted in the formation of a strong Hg—O bond. However, these reactive O atoms are not available when  $H_2$  is present in the gas phase, as the metal oxide is reduced to an inactive form in  $H_2$  atmosphere. Therefore, metal oxides are not suitable as Hg sorbents in reducing fuel gas atmosphere, as is the case for coal fuel gas.

It was surprisingly found that supported  $CuO$  sorbents had high Hg-sorption capacity even in the presence of  $H_2$ , provided the gas also contained  $H_2S$ . It is theorized that Cu atoms in such supported sorbents are in “dispersed” form, with two Cu atoms separated by a longer distance compared to a “bulk”  $CuO$  sorbent. Due to the dispersed nature of the Cu atoms, when exposed to  $H_2$  and  $H_2S$ , the sorbent does not form  $Cu_2S$ , the formation of which requires two Cu atoms separated by a certain fixed distance. In such a situation, dispersed Cu sorbent forms  $CuS$ , which is much more reactive for Hg capture than  $Cu_2S$ . The presence of  $H_2S$  in the gas phase helps in keeping the reactive S atoms attached to the Cu atoms on the support. The reactive S atoms, in turn, capture gas phase Hg by chemisorption mechanism. It was also found that the captured Hg on such supported sorbents could be easily released when the spent sorbent is exposed to a SFG stream that is cleaned of Hg and S components.

Based on this novel mechanism of mercury capture, a process can be devised in which Hg from coal fuel gas is captured on supported/dispersed Cu-based sorbents by contacting the sorbent and fuel gas upstream of the desulfurization unit. After the sorbent is spent, it is regenerated by exposing the sorbent to a smaller gas stream containing  $H_2$  gas, such as that coming out of the desulfurization unit in the plant. The released Hg, which is in much higher concentrated form and in lower volume of gas, can be captured using a sulfur-impregnated activated carbon maintained at room temperature. The exit stream of the low-temperature Hg-capture unit, which now contains much lower concentration of Hg, can be sent back to the mercury capture unit at the high temperature. The proposed process allows for the fuel gas stream to be maintained at high temperature, thus maintaining thermodynamic efficiency of the process.

This study has demonstrated that supported nanocrystalline Cu-based sorbents have potential to capture mercury from coal fuel gas at high temperatures. Since  $CuS$ -based sorbents are known to capture arsenic as well, further studies are recommended to synthesize supported Cu-sorbents with higher Cu loadings and evaluate their potential to remove arsenic and selenium from coal fuel gas in a regenerative manner. Development of such multifunctional and regenerable sorbents can drastically reduce the overall cost of trace element capture.